Contribution from the Laboratoire de Synthèse et d'Electrosynthèse Organométalliques, associé au CNRS (URA 33), Faculté des Sciences "Gabriel", 6, Boulevard Gabriel, 21100 Dijon, France, Department of Chemistry, University of Houston, Houston, Texas 77204-5641, and Laboratoire de Minéralogie et Cristallographie associé au CNRS (URA 809), Université de Nancy I, BP 239, 54506 Vandoeuvre les Nancy, France

Metalloporphyrins Containing σ-Bonded Nitrogen Axial Ligands. 1. Synthesis and Characterization of Indium(III) Porphyrin Complexes. Molecular Structures of (4-Phenyltetrazolato)- and (5-Methyltetrazolato)(2,3,7,8,12,13,17,18-octaethylporphinato)indium(III)

R. Guilard,*[1a] N. Jagerovic,[1a] A. Tabard,[1a] P. Richard,[1a] L. Courthaudon,[1b] A. Louati,[1b,c] C. Lecomte,*[1d] and K. M. Kadish*[1b]

Received June 11, 1990

The synthesis and characterization of 16 nitrogen σ-bonded (tetrazolato)- and (triazolato)indium(III) porphyrin complexes are reported. Each metalloporphyrin was characterized by UV-visible, IR, and ^{1}H NMR spectroscopy as well as by electrochemistry. The molecular structure of (OEP)In[$N_4C(CH_3)$] was solved and compared to (OEP)In[$N_4C(C_6H_5)$], whose characterization was reported in a preliminary communication. (OEP)In[$N_4C(CH_3)$] crystallizes in the triclinic system, space group $P\bar{1}$ (a = 12.035 (2) Å, b = 12.855 (2) Å, c = 14.097 (3) Å, α = 110.00 (3)°, β = 111.10 (3)°, γ = 90.52 (3)°, Z = 2, ρ = 1.265 g cm^{-3}, $R(F)$ = 5.13%). The tetrazolato group of (OEP)In[$N_4C(CH_3)$] is substituted at the 5-position of the axial ligand, whereas the C_6H_5 group of (OEP)In[$N_4C(C_6H_5)$] is substituted in the 4-position of the tetrazolato ligand. The spectroscopic data suggest that the tetrazole or triazole linkage mode depends upon the nature of the aryl or alkyl group attached to the axial ligand, and this was confirmed by structural data for two of the complexes.

Introduction

The 1,3-dipolar cycloaddition of organic azides to dipolarophiles such as nitriles or alkynes is known to produce tetrazolato or triazolato derivatives.[2-6] An azido group coordinated to a metalloporphyrin can also undergo this cycloaddition reaction and will give the metalloporphyrin that is coordinated to a tetrazolato or triazolato axial ligand.[7-10] These reactions can lead to two different isomers, as shown in Chart I for the case of (P)In[$N_4C(R)$] where P = the dianion of a given porphyrin ring[11] and R is a given alkyl or aryl group.[3,12,13]

A single-crystal X-ray analysis of (OEP)In[$N_4C(C_6H_5)$] was reported in a preliminary communication[7] and gave the thermodynamic product corresponding to isomer II. However, it was not known if the same type of isomer would also be obtained from reactions involving (OEP)InN_3 and other organic nitriles. This is investigated in the present paper, which presents an X-ray structure of (OEP)In[$N_4C(CH_3)$] and demonstrates that isomer I is isolated in the reaction between (OEP)InN_3 and CH_3CN. This paper also gives a complete spectroscopic and electrochemical characterization of the (tetrazolato)indium(III) products generated from (P)InN_3 where P = OEP, TPP, or Tp-CF_3PP and the nitrile p-$NO_2C_6H_4CN$, C_6H_5CN, CH_3CH_2CN, or CH_3CN.

Chart I

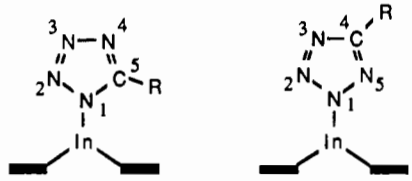

Chart II

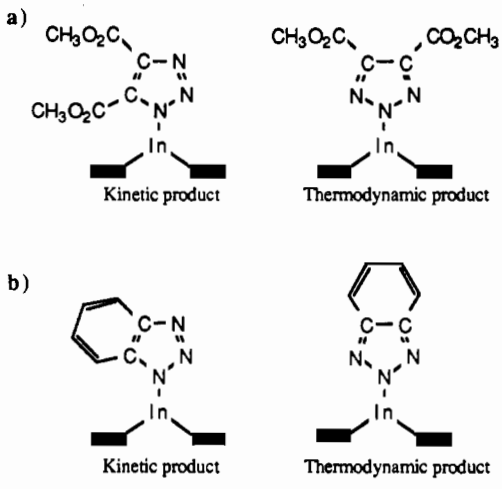

The formation of a triazolato complex from an alkyne and an azido group coordinated to a metal is also known in organometallic chemistry,[12-19] and (P)InN_3 exhibits a similar reactivity toward dipolarophiles such as alkynes. Two isomers can also be isolated

(1) (a) Université de Bourgogne. (b) University of Houston. (c) On leave of absence from Université Louis Pasteur, Strasbourg, France. (d) Université de Nancy.
(2) Huisgen, R. *Angew. Chem., Int. Ed. Engl.* **1963**, *2*, 633.
(3) L'Abbé, G. *Chem. Rev.* **1969**, *69*, 345.
(4) Patai, S. *The Chemistry of Azido Group*; Interscience: New York, 1971.
(5) Huisgen, R. In *1,3-Dipolar Cycloaddition Chemistry*; Padwa, A., Ed.; Interscience: New York, 1984; Vol. 1, Chapter 1.
(6) Scriven, E. F. V. *Azides and Nitrenes, Reactivity and Utility*; Academic Press: Orlando, FL, 1984.
(7) Guilard, R.; Gerges, S. S.; Tabard, A.; Richard, P.; El Borai, M. A.; Lecomte, C. *J. Am. Chem. Soc.* **1987**, *109*, 7228.
(8) Geisenberger, J.; Erbe, J.; Heidrich, J.; Nagel, U.; Beck, W. *Z. Naturforsch.* **1987**, *42B*, 55.
(9) Guilard, R.; Perrot, I.; Tabard, A.; Richard, P.; Lecomte, C.; Liu, Y.-H.; Kadish, K. M. *Inorg. Chem.*, following paper in this issue.
(10) Jagerovic, N.; Barbe, J.-M.; Farnier, M.; Guilard, R. *J. Chem. Soc., Dalton Trans.* **1988**, 2569.
(11) Abbreviations: P = any porphyrin; (OEP)H_2 = octaethylporphyrin; (TPP)H_2 = tetraphenylporphyrin; (Tp-CF_3PP)H_2 = tetrakis(p-(trifluoromethyl)phenyl)porphyrin.
(12) Kemmerich, T.; Nelson, J. H.; Takach, N. E.; Boehme, H.; Jablonski, B.; Beck, W. *Inorg. Chem.* **1982**, *21*, 1226.
(13) Paul, P.; Nag, K. *Inorg. Chem.* **1987**, *26*, 2969.
(14) Kozima, S.; Itano, T.; Mihara, N.; Sisido, K.; Isida, T. *J. Organomet. Chem.* **1972**, *44*, 117.
(15) Gorth, H.; Henry, M. C. *J. Organomet. Chem.* **1967**, *9*, 117.
(16) Kemmerich, T.; Beck, W.; Spencer, C.; Mason, R. *Z. Naturforsch.* **1972**, *27B*, 715.
(17) Rigby, W.; Bailey, P. M.; McCleverty, J. A.; Maitlis, P. M. *J. Chem. Soc., Dalton Trans.* **1979**, 371.
(18) Kreutzer, P. H.; Weis, J. C.; Bock, H.; Erbe, J.; Beck, W. *Chem. Ber.* **1983**, *116*, 2691.
(19) Rosan, A.; Rosenblum, M. *J. Organomet. Chem.* **1974**, *80*, 103.

0020-1669/91/1330-0016$02.50/0

Table I. Yields, Elemental Analyses, and Mass Spectral Data for the Tetrazolato and Triazolato Complexes

porphyrin, P	axial ligand	molecular formula	yield, %	anal.[a] % C	% H	% N
OEP	$N_4C(CH_3)$	$C_{38}H_{47}N_8In$	67	62.5 (62.5)	6.4 (6.5)	14.8 (15.3)
	$N_4C(CH_2CH_3)$	$C_{39}H_{49}N_8In$	69	62.9 (62.9)	6.6 (6.6)	14.2 (15.0)
	$N_4C(C_6H_5)$	$C_{43}H_{49}N_8In$	55	65.2 (65.1)	6.1 (6.2)	13.6 (14.1)
	$N_4C(p\text{-}NO_2C_6H_4)$	$C_{43}H_{48}N_9InO_2$	88	61.1 (61.6)	5.7 (5.8)	13.6 (15.3)
	$N_3C_2(CO_2CH_3)_2$	$C_{42}H_{50}N_7InO_4$	69	59.4 (60.6)	6.0 (6.1)	11.1 (11.8)
	$N_3C_6H_4$	$C_{42}H_{48}N_7In$	51	64.5 (65.9)	6.8 (6.3)	12.1 (12.8)
TPP	$N_4C(CH_3)$	$C_{46}H_{31}N_8In$	49	67.3 (68.2)	3.7 (3.9)	13.0 (13.8)
	$N_4C(CH_2CH_3)$	$C_{47}H_{33}N_8In$	65	68.4 (68.5)	3.9 (4.0)	13.4 (13.6)
	$N_4C(C_6H_5)$	$C_{51}H_{33}N_8In$	65	69.6 (70.2)	3.9 (3.8)	12.5 (12.8)
	$N_4C(p\text{-}NO_2C_6H_4)$	$C_{51}H_{32}N_9InO_2$	59	66.7 (66.7)	3.5 (3.5)	12.9 (13.7)
	$N_3C_2(CO_2CH_3)_2$	$C_{50}H_{34}N_7InO_4$	61	66.0 (65.9)	4.6 (3.8)	9.5 (10.7)
Tp-CF_3PP	$N_4C(CH_3)$	$C_{50}H_{27}N_8InF_{12}$	58	55.2 (55.5)	2.6 (2.5)	10.2 (10.3)
	$N_4C(CH_2CH_3)$	$C_{51}H_{29}N_8InF_{12}$	57	56.6 (55.9)	2.7 (2.7)	9.3 (10.2)
	$N_4C(C_6H_5)$	$C_{55}H_{29}N_8InF_{12}$	32	57.3 (57.7)	2.6 (2.6)	9.9 (9.8)
	$N_4C(p\text{-}NO_2C_6H_4)$	$C_{55}H_{28}N_9InO_2F_{12}$	48	55.8 (55.5)	2.4 (2.4)	9.8 (10.6)
	$N_3C_2(CO_2CH_3)_2$	$C_{54}H_{30}N_7InO_4F_{12}$	47	54.2 (54.8)	2.8 (2.6)	7.9 (8.3)

[a] Calculated values in parentheses.

from these reactions and, for the case of dimethyl acetylenedicarboxylate or benzyne, will correspond to either a thermodynamic or kinetic product, as shown in Chart II. The synthesis and characterization of these triazolato complexes are detailed in the present paper, which provides the first example for the addition of benzyne to an azido metallo complex.

Altogether 16 different σ-bonded triazolato and tetrazolato complexes are characterized in this paper by UV–visible, IR, and ^{1}H NMR spectroscopy, X-ray structural analysis, and electrochemistry. These results are analyzed with respect to the formation of a kinetic or a thermodynamic product and are also compared to data reported in the literature for related In(III) porphyrins with either σ-bonded carbon or ionic axial ligands.

Experimental Section

Chemicals. The synthesis and handling of each porphyrin were carried out under an argon atmosphere. Acetonitrile, benzonitrile, propionitrile, and dimethyl acetylenedicarboxylate were freshly distilled under an inert atmosphere. Commercial grade *p*-nitrobenzonitrile was used without further purification. Benzyne was prepared in situ by using a literature method.[20] Reagent grade methylene chloride (CH_2Cl_2, Fisher) was distilled over P_2O_5 for electrochemical studies. Tetrabutylammonium hexafluorophosphate ((TBA)PF_6) and tetrabutylammonium perchlorate ((TBA)ClO_4) were purchased from Fluka and recrystallized from ethanol prior to use.

(P)InCl derivatives were obtained by metalation of the corresponding free-base porphyrins, (P)H_2, using literature methods for (OEP)InCl,[21a] (TPP)InCl,[21b] and (Tp-CF_3PP)InCl.[21a] The starting (P)InN_3 derivatives were synthesized from (P)InCl according to the general procedure described below.

Synthesis and Characterization of (P)InN_3 Where P = OEP, TPP, or Tp-CF_3PP. To a solution of (P)InCl (0.55 mmol) in methylene chloride was added NaN_3 (18.5 mmol). The reaction mixture was stirred for 12 h at room temperature, after which the solution was filtered and the solvent removed in vacuo. The crude product was recrystallized from toluene to give a final yield close to 60% for all of the investigated (P)InN_3 complexes. UV–visible (THF) [λ_{max}, nm ($10^{-3}\epsilon$, M^{-1} cm^{-1})]: (OEP)InN_3 386 (50.6), 408 (314.6), 498 (1.0), 539 (16.4), 577 (17.1); (TPP)InN_3 403 (42.7), 425 (561.5), 522 (1.9), 561 (18.5), 601 (9.8); (Tp-CF_3PP)InN_3 404 (48.1), 425 (520.8), 520 (2.5), 560 (20.8), 600 (8.3).

Synthesis and Preparation of (P)In[$N_4C(R)$] Where R = CH_3, CH_2CH_3, C_6H_5, or p-$NO_2C_6H_4$ and P = OEP, TPP, or Tp-CF_3PP. (P)InN_3 (200 mg) was mixed with acetonitrile (30 mL), propionitrile (20 mL), benzonitrile (30 mL), or *p*-nitrobenzonitrile (100 mg) and 10 mL of toluene (or 10 mL of methylene chloride for the case where P = OEP). The mixture was refluxed for about 4 h and the progress of the reaction monitored by observing the disappearance of the N_3^- band at 2070 cm^{-1} by IR spectroscopy. The solution was then evaporated and the resulting crude solid recrystallized from toluene. The reaction yields varied from 32 to 88% and are summarized in Table I.

Synthesis of (P)In[$N_3C_2(CO_2CH_3)_2$] Where P = OEP, TPP, or Tp-CF_3PP. Freshly distilled dimethyl acetylenedicarboxylate (40 μL, 0.33 mmol) was added to a solution containing 150 mg (0.22 mmol) of (OEP)InN_3 in 50 mL of toluene. The mixture was refluxed for 3 h as the N_3^- vibration at 2070 cm^{-1} disappeared. The solution was evaporated and the solid recrystallized from a 2/1 toluene/heptane mixture to give 120 mg of (OEP)In[$N_3C_2(CO_2CH_3)_2$] (yield = 69%). The other (P)-In[$N_3C_2(CO_2CH_3)_2$] complexes were synthesized by using the same procedure and gave the overall yields summarized in Table I.

Synthesis of (OEP)In($N_3C_6H_4$). Anthranilic acid (43 mg, 0.31 mmol) in 10 mL of acetone was added slowly to a solution containing 30 mL of methylene chloride, 39 mg of isoamyl nitrite (0.33 mmol), and 200 mg of (OEP)InN_3 (0.29 mmol). The mixture was stirred at 120 °C for 3 h. The completion of the reaction was ascertained by the disappearance of the N_3^- vibration at 2070 cm^{-1}. The solvent was evaporated, and recrystallization of the resulting solid in toluene gave 170 mg of (OEP)In($N_3C_6H_4$) (yield = 51%).

Physicochemical Measurements. Elemental analyses were performed by the Service de Microanalyse of the CNRS. ^{1}H NMR spectra were recorded at 400 MHz on a Bruker WM 400 spectrometer of CEREMA (Centre de Résonance Magnétique de l'Université de Bourgogne). Spectra were measured from 5-mg solutions of the complex in deuterated solvents with tetramethylsilane as internal reference. ESR spectra were recorded in 115 K on an IBM Model ER 100D spectrometer equipped with a Model ER-040-X microwave bridge and a Model ER 080 power supply. The g values were measured with respect to diphenylpicrylhydrazyl (g = 2.0036 ± 0.0003). Infrared spectra were obtained on a Perkin-Elmer 580 B apparatus. Solid samples were prepared as 1% dispersions in a CsI pellet. Electronic absorption spectra were recorded on a Perkin-Elmer 559 spectrophotometer, an IBM Model 9430 spectrophotometer, or a Tracor Northern 1710 holographic optical spectrophotometer–multichannel analyzer.

Cyclic voltammograms were obtained with the use of a three-electrode system. The working electrode was a platinum button, and a platinum wire was used as the counter electrode. A saturated calomel electrode (SCE) served as the reference electrode and was separated from the bulk of the solution by a fritted-glass bridge. A BAS 100 electrochemical analyzer connected to a Houston Instruments HIPLOT DMP 40 plotter was used to measure the current–voltage curves.

Controlled-potential electrolysis was performed with an EG&G Model 173 potentiostat or a BAS 100 electrochemical analyzer. Both the reference electrode and the platinum-wire counter electrode were separated from the bulk of the solution by means of a fritted-glass bridge. Thin-layer spectroelectrochemical measurements were performed with an IBM EC 225 voltammetric analyzer coupled with a Tracor Northern 1710 spectrophotometer–multichannel analyzer to give time-resolved spectral data. The utilized optically transparent platinum thin-layer electrode (OTTLE) is described in the literature.[22]

Crystal and Molecular Structure of (OEP)In[$N_4C(C_6H_5)$] and (OEP)In[$N_4C(CH_3)$]. Experimental conditions and the crystal structure determination of (OEP)In[$N_4C(C_6H_5)$] are reported in a preliminary

(20) Banks, R. E.; Higgons, R. I.; Prakash, A.; Rawston, M.; Sparkes, G. R. *J. Fluorine Chem.* **1977**, *9*, 327.

(21) (a) Eaton, S. S.; Eaton, G. R. *J. Am. Chem. Soc.* **1975**, *97*, 3660. (b) Bhatti, M.; Bhatti, W.; Mast, E. *Inorg. Nucl. Chem. Lett.* **1972**, *8*, 133.

(22) Lin, X. Q.; Kadish, K. M. *Anal. Chem.* **1985**, *57*, 1498.

Table II. Experimental Conditions[a]

compd	(OEP)In[$N_4C(CH_3)$]
formula	$C_{38}H_{47}N_8In$
fw	730.70
space group	triclinic, $P\bar{1}$
lattice params	
a, b, c, Å	12.035 (2), 12.855 (2), 14.097 (3)
α, β, γ, deg	110.00 (3), 111.10 (3), 90.52 (3)
V, Å^3; Z; ρ_{calcd}, g cm^{-3}	1917.3; 2; 1.265
$F(000)$	760
diffractometer	Enraf-Nonius CAD 4F (room temp)
radiation	Mo Kα (graphite monochromatized)
scan type (sin θ)/λ_{max}, Å^{-1}	ω–2θ; 0.68
scan range, deg; scan speed, deg min^{-1}	1 + 0.35 tan θ; 0.2 < v < 2.0
aperture, mm	4
no. of rflns measd	5314
no. of rflns used (N)	4229
no. of params (N_p)	424
N/N_p	9.97
program used	SDP,[23] SHELX 76[24]
$R(F)$, %	5.13
$R_w(F)$, %	5.13
GOF	3.70

[a] Experimental conditions for (OEP)In[$N_4C(C_6H_5)$] are given in ref 7.

communication.[7] Suitable crystals of (OEP)In[$N_4C(CH_3)$] were obtained from recrystallization in toluene. Weissenberg photographs of (OEP)In[$N_4C(CH_3)$] revealed a triclinic cell. Experimental conditions are given in Table II. A total of 5314 reflections were collected at room temperature, and 4229 reflections ($I \geq 3\sigma(I)$) were used. The structure was solved by interpretation of the Patterson map and refined in the centrosymmetric space group via standard least-squares and Fourier techniques. All non-hydrogen atoms were refined anisotropically, and hydrogen fractional coordinates were calculated. The final residual for 424 variables gave $R(F) = 5.13\%$ (unit weight scheme). Scattering factors were taken from refs 24 and 25. Fractional coordinates for the non-hydrogen atoms of (OEP)In[$N_4C(C_6H_5)$] and (OEP)In[$N_4C(CH_3)$] are given in Tables III and IV, while main bond distances and angles are given in Table V. A list of other bond distances and angles, anisotropic thermal parameters, hydrogen coordinates, least-squares planes, and structure factors for (OEP)In[$N_4C(CH_3)$] are given as supplementary material.

Results and Discussion

Characterization of Neutral (P)In[$N_4C(R)$] Complexes. Twelve σ-bonded tetrazolato complexes were synthesized from the corresponding (P)InN_3 derivatives. The overall reaction involves a cycloaddition of the bound azido group on (P)InN_3 with *p*-$NO_2C_6H_4CN$, C_6H_5CN, CH_3CN, or CH_3CH_2CN, as described in the Experimental Section.

The formation of (P)In[$N_4C(R)$] was determined by monitoring the disappearance of the N_3^- vibrational bands during the reaction. The rate of this reaction was fastest when *p*-$NO_2C_6H_4CN$ was the dipolarophile, and this is consistent with the electron-withdrawing properties of the nitrile; i.e. the least electron-rich nitrile is the most reactive. In contrast, the cycloaddition reaction did not appear to depend upon the nature of the porphyrin macrocycle and this can be explained by the lack of an equatorial ligand influence on the polarizability of the azido group.

Infrared data for the various (P)In[$N_4C(R)$] species are summarized in Table VI, which lists only those vibrational frequencies not found in the starting (P)InN_3 derivatives. As expected, the symmetric and antisymmetric N_3^- bands disappear as new vibrations attributed to the axially complexed tetrazolato axial ligand appear. The tetrazole ring deformations exhibit typical[18,26-30] vibrational frequencies in the range 984–1503 cm^{-1} (see Table VI). Other IR bands at higher wavenumbers are due to the alkyl or aryl substituent on the tetrazolato ligand.

Phenyl vibrations for the tetrazole ring of (P)In[$N_4C(C_6H_5)$] appear at 3066–3070 cm^{-1}, while the antisymmetric and symmetric nitro stretching frequencies of (P)In[$N_4C(p\text{-}NO_2C_6H_4)$] are located in the ranges 1510–1521 and 1337–1350 cm^{-1}.[31] An assignment of the vibrational frequencies in the 498–880-cm^{-1} region is not definitive, but these bands seem to be associated with the tetrazole ring or its R substituent group. A broad band characteristic of the indium–nitrogen vibrator[29] is also observed around 300 cm^{-1} for four of the complexes.

Table III. Fractional Coordinates, Standard Deviations, and Equivalent Isotopic Temperature Factors (Å^2) of (4-Phenyltetrazolato)(2,3,7,8,12,13,17,18-octaethylporphinato)-indium(III)

atom	x	y	z	B
In	0.13650 (3)	0.02835 (3)	0.07398 (2)	3.211 (6)
N1	0.1961 (3)	−0.0272 (4)	−0.0077 (2)	3.42 (9)
N2	0.2286 (3)	0.1663 (4)	0.0520 (2)	3.30 (9)
N3	0.0375 (3)	0.1219 (3)	0.1347 (2)	3.4 (1)
N4	0.0044 (3)	−0.0721 (4)	0.0748 (2)	3.5 (1)
N5	0.2354 (4)	−0.0642 (4)	0.1192 (2)	4.0 (1)
N6	0.2860 (5)	−0.1471 (5)	0.0977 (2)	7.7 (2)
N7	0.3503 (5)	−0.1767 (5)	0.1313 (2)	8.1 (2)
N8	0.2649 (4)	−0.0362 (4)	0.1652 (2)	4.5 (1)
C1	0.1670 (4)	−0.1189 (4)	0.0292 (2)	3.5 (1)
C2	0.2448 (4)	−0.1476 (5)	−0.0772 (2)	3.7 (1)
C3	0.3198 (4)	−0.0714 (5)	−0.0843 (2)	3.7 (1)
C4	0.2893 (4)	0.0044 (4)	−0.0402 (2)	3.4 (1)
C5	0.3429 (4)	0.0964 (5)	−0.0311 (2)	3.8 (1)
C6	0.3148 (4)	0.1724 (4)	0.0101 (2)	3.3 (1)
C7	0.3691 (4)	0.2705 (5)	0.0154 (2)	3.5 (1)
C8	0.3131 (4)	0.3227 (4)	0.0597 (2)	3.4 (1)
C9	0.2248 (4)	0.2559 (4)	0.0831 (2)	3.4 (1)
C10	0.1486 (4)	0.2787 (5)	0.1297 (2)	3.7 (1)
C11	0.0618 (4)	0.2187 (4)	0.1538 (2)	3.5 (1)
C12	−0.0186 (5)	0.2473 (5)	0.2008 (2)	4.0 (1)
C13	−0.0895 (4)	0.1680 (5)	0.2091 (2)	4.0 (1)
C14	−0.0551 (4)	0.0889 (5)	0.1675 (2)	3.7 (1)
C15	−0.1067 (4)	−0.0043 (4)	0.1589 (2)	4.0 (1)
C16	−0.0813 (4)	−0.0788 (4)	0.1173 (2)	3.5 (1)
C17	−0.1381 (4)	−0.1736 (5)	0.1100 (2)	4.2 (1)
C18	−0.0886 (4)	−0.2207 (5)	0.0634 (2)	3.9 (1)
C19	0.0021 (4)	−0.1568 (5)	0.0410 (2)	3.7 (1)
C20	0.0767 (4)	−0.1777 (5)	−0.0070 (2)	3.9 (1)
C25	0.2423 (8)	−0.2472 (5)	−0.1100 (2)	4.7 (1)
C26	0.2770 (6)	−0.3430 (6)	−0.0812 (3)	6.5 (2)
C27	0.4196 (1)	−0.0657 (5)	−0.1268 (2)	4.5 (1)
C28	0.5123 (5)	−0.1163 (7)	−0.1069 (3)	6.5 (2)
C29	0.4701 (4)	0.3040 (5)	−0.0223 (2)	4.4 (1)
C30	0.4530 (5)	0.3576 (6)	−0.0748 (3)	5.8 (2)
C31	0.3317 (5)	0.4317 (5)	0.0783 (3)	4.6 (1)
C32	0.2698 (6)	0.5133 (6)	0.0544 (3)	6.7 (2)
C33	−0.0232 (5)	0.3500 (5)	0.2311 (2)	4.8 (1)
C34	−0.0770 (6)	0.4357 (6)	0.2049 (3)	6.8 (2)
C35	−0.1901 (5)	0.1628 (6)	0.2515 (3)	5.6 (2)
C36	−0.1789 (8)	0.1089 (8)	0.3035 (4)	11.4 (3)
C37	−0.2349 (5)	−0.2100 (6)	0.1499 (3)	5.5 (2)
C38	−0.2066 (7)	−0.2665 (7)	0.1997 (4)	8.6 (2)
C39	−0.1142 (5)	−0.3247 (5)	0.0392 (3)	5.3 (2)
C40	−0.0606 (7)	−0.4161 (6)	0.0612 (4)	7.9 (2)
C41	0.3361 (4)	−0.1073 (5)	0.1724 (2)	4.2 (1)
C42	0.3944 (5)	−0.1090 (6)	0.2176 (2)	4.8 (1)
C43	0.3890 (6)	−0.0247 (8)	0.2525 (3)	7.8 (2)
C44	0.4470 (8)	−0.025 (1)	0.2940 (3)	12.0 (3)
C45	0.5072 (7)	−0.109 (1)	0.3018 (3)	12.9 (4)
C46	0.5119 (7)	−0.195 (1)	0.2682 (3)	10.6 (3)
C47	0.4553 (6)	−0.1956 (8)	0.2255 (3)	7.3 (2)

(23) *SDP: Structure Determination Package*; Enraf-Nonius: Delft, The Netherlands, 1977.
(24) Sheldrick, G. M. *SHELX 76: Program for Crystal Structure Determinations*; University of Göttingen: Göttingen, FRG, 1976.
(25) *International Tables for X-Ray Crystallography*; Kynoch: Birmingham, U.K., 1974; Vol. IV.
(26) Lieber, E.; Levering, D. R.; Patterson, L. J. *Anal. Chem.* **1951**, *23*, 1594.
(27) Jonassen, H. B.; Terry, J. O.; Harris, A. D. *J. Inorg. Nucl. Chem.* **1963**, *25*, 1239.
(28) Holm, R. D.; Donnely, P. L. *J. Inorg. Nucl. Chem.* **1966**, *28*, 1887.
(29) Garber, L. L.; Sims, L. B.; Brubaker, C. H., Jr. *J. Am. Chem. Soc.* **1968**, *90*, 2518.
(30) Beck, W.; Fehlhammer, W. P.; Bock, H.; Bauder, M. *Chem. Ber.* **1969**, *102*, 3637.
(31) Bellamy, L. J. *The Infrared Spectra of Complex Molecules*, 2nd ed.; Chapman and Hall: London, 1980; Vol. II, p 229.

Table IV. Fractional Coordinates, Standard Deviations, and Equivalent Isotopic Temperature Factors (Å^2) of (5-Methyltetrazolato)(2,3,7,8,12,13,17,18-octaethylporphinato)-indium(III)

atom	*x*	*y*	*z*	*B*
In	0.56742 (5)	0.33690 (5)	0.71695 (4)	3.03 (1)
N1	0.7107 (5)	0.3006 (5)	0.8345 (4)	3.6 (2)
N2	0.6997 (5)	0.3733 (5)	0.6611 (4)	3.4 (2)
N3	0.4385 (5)	0.2972 (5)	0.5569 (4)	3.2 (2)
N4	0.4487 (5)	0.2247 (5)	0.7316 (4)	3.2 (2)
N5	0.5323 (6)	0.4991 (5)	0.8097 (5)	4.1 (2)
N6	0.507 (1)	0.6513 (8)	0.9225 (8)	8.3 (4)
N7	0.431 (1)	0.6346 (8)	0.8222 (9)	8.7 (4)
N8	0.4467 (8)	0.5444 (7)	0.7542 (6)	6.7 (3)
C1	0.6974 (7)	0.2531 (6)	0.9038 (6)	3.6 (2)
C2	0.8170 (7)	0.2559 (6)	0.9804 (6)	3.8 (2)
C3	0.8993 (7)	0.3040 (6)	0.9578 (6)	3.7 (2)
C4	0.8320 (6)	0.3327 (6)	0.8655 (6)	3.8 (2)
C5	0.8803 (7)	0.3821 (6)	0.8146 (6)	4.0 (2)
C6	0.8214 (6)	0.3990 (6)	0.7191 (6)	3.7 (2)
C7	0.8788 (7)	0.4401 (6)	0.6632 (7)	4.3 (2)
C8	0.7899 (7)	0.4331 (6)	0.5696 (6)	3.9 (2)
C9	0.6770 (6)	0.3924 (6)	0.5681 (6)	3.4 (2)
C10	0.5638 (7)	0.3725 (6)	0.4873 (6)	3.6 (2)
C11	0.4544 (6)	0.3275 (6)	0.4797 (5)	3.2 (2)
C12	0.3394 (7)	0.3024 (6)	0.3907 (5)	3.6 (2)
C13	0.2558 (7)	0.2581 (7)	0.4158 (6)	3.9 (2)
C14	0.3195 (6)	0.2526 (6)	0.5204 (5)	3.2 (2)
C15	0.2704 (6)	0.2063 (6)	0.5736 (6)	3.5 (2)
C16	0.3287 (6)	0.1902 (6)	0.6684 (5)	3.0 (2)
C17	0.2758 (6)	0.1307 (6)	0.7154 (6)	3.7 (2)
C18	0.3661 (7)	0.1305 (6)	0.8059 (6)	3.6 (2)
C19	0.4753 (6)	0.1896 (6)	0.8164 (5)	3.3 (2)
C20	0.5888 (7)	0.2066 (6)	0.8951 (5)	3.7 (2)
C25	0.8393 (8)	0.2073 (7)	1.0643 (6)	5.1 (3)
C26	0.833 (1)	0.084 (1)	1.0208 (9)	8.5 (4)
C27	1.0335 (7)	0.3198 (7)	1.0094 (6)	4.7 (3)
C28	1.0832 (9)	0.2239 (9)	0.9439 (9)	7.7 (4)
C29	1.0118 (7)	0.4781 (8)	0.7033 (8)	5.7 (3)
C30	1.080 (1)	0.385 (1)	0.677 (1)	9.3 (5)
C31	0.8023 (8)	0.4551 (7)	0.4780 (7)	5.1 (3)
C32	0.8071 (9)	0.3478 (8)	0.3898 (8)	6.8 (3)
C33	0.3201 (7)	0.3197 (7)	0.2879 (6)	4.9 (3)
C34	0.348 (1)	0.2202 (9)	0.2082 (8)	8.0 (4)
C35	0.1228 (8)	0.217 (1)	0.3492 (7)	6.8 (4)
C36	0.095 (1)	0.089 (1)	0.2819 (9)	8.6 (4)
C37	0.1477 (7)	0.0748 (7)	0.6681 (7)	5.1 (3)
C38	0.127 (1)	−0.044 (1)	0.589 (1)	8.4 (4)
C39	0.3594 (7)	0.0768 (7)	0.8801 (6)	4.5 (3)
C40	0.401 (1)	−0.0393 (8)	0.8532 (7)	6.8 (3)
C41	0.5657 (9)	0.5674 (8)	0.9128 (7)	5.4 (3)
C42	0.659 (1)	0.548 (1)	1.0048 (8)	8.1 (4)

Table V. Main Bond Distances (Å), Angles (deg), and Standard Deviations of (OEP)In[$N_4C(CH_3)$] and (OEP)In[$N_4C(C_6H_5)$]

	(OEP)In[$N_4C(CH_3)$]		
In–N1	2.130 (6)	N5–N8	1.34 (1)
In–N2	2.140 (7)	N5–C41	1.33 (2)
In–N3	2.133 (5)	N6–N7	1.35 (1)
In–N4	2.137 (8)	N6–C41	1.28 (2)
In–N5	2.177 (6)	N7–N8	1.29 (1)
N1–In–N2	86.6 (3)	N4–In–N5	100.5 (3)
N1–In–N3	152.7 (2)	N8–N5–C41	105.5 (7)
N1–In–N4	87.0 (2)	N7–N6–C41	105.9 (9)
N2–In–N3	86.6 (2)	N6–N7–N8	110 (1)
N2–In–N4	153.1 (2)	N5–N8–N7	108.1 (8)
N3–In–N4	87.3 (2)	N5–C41–N6	110.9 (9)
N1–In–N5	103.6 (2)	N5–C41–C42	124 (1)
N2–In–N5	106.4 (3)	N6–C41–C42	125.1 (9)
N3–In–N5	103.7 (2)		
	(OEP)In[$N_4C(C_6H_5)$]		
In–N1	2.126 (4)	N5–N8	1.303 (7)
In–N2	2.129 (4)	N5–N6	1.298 (8)
In–N3	2.132 (4)	N7–C41	1.324 (9)
In–N4	2.125 (4)	N7–N6	1.33 (1)
In–N5	2.183 (5)	C41–N8	1.322 (8)
N1–In–N2	87.0 (2)	N4–In–N5	102.4 (2)
N1–In–N3	155.0 (2)	N8–N5–N6	111.6 (5)
N1–In–N4	87.6 (2)	N6–N7–C41	105.7 (6)
N2–In–N3	87.2 (2)	N7–C41–N8	110.7 (6)
N2–In–N4	154.8 (2)	N5–N8–C41	104.5 (5)
N3–In–N4	87.3 (2)	N5–N6–N7	107.5 (6)
N1–In–N5	99.0 (2)	N8–C41–C42	125.7 (6)
N2–In–N5	102.7 (2)	N7–C41–C42	123.6 (6)
N3–In–N5	106.0 (2)		

A summary of the UV–visible data for each In(III) species, including the starting (P)InN_3 derivatives, is given Table VII. The electronic absorption spectra of (P)In[$N_4C(R)$] have two absorption bands (labeled (B(1,0) and B(0,0)) in the range 384–425 nm and three Q bands in the range 496–601 nm. The spectra of (P)In[$N_4C(R)$] belong to the normal porphyrin class[32] and closely resemble the UV–visible spectra of ionic (P)InN_3. In contrast, these spectra differ from those of In–carbon σ-bonded complexes of the type (P)In(R)[33,34] and this is consistent with the anionic character of the tetrazole ring.

The data in Table VII show that the $\pi \rightarrow \pi^*$ electronic transition (the B(0,0) or Soret band) is not related to the nature of the axial ligand but rather depends upon the electron donicity of the porphyrin macrocycle. The Soret bands of the four tetrazolato OEP complexes are blue-shifted by about 18 nm compared to the Soret bands of the four TPP derivatives with the same σ-bonded axial ligands.

A tetrazolato group can be coordinated to metal complexes in several different ways. One involves unidentate coordination, where the linkage to the metal is via one of the two modes shown in Chart I. Another type of linkage involves ambidentate bonding.[35-37] IR and UV–visible data for the (P)In[$N_4C(R)$] complexes indicate the absence of ambidentate bonding and the presence of only a single isomer of the type shown in Chart I. However, the spectroscopic data do not indicate if the axially coordinated ligand is substituted at the 4- or 5-position of the tetrazole ring; i.e. it does not indicate the type of isomer in the (P)In[$N_4C(R)$] complex.

Table VIII summarizes ^{1}H NMR data for (P)InN_3 and (P)-In[$N_4C(R)$] in hexadeuteriobenzene. The chemical shifts of the tetrazolato complexes are close to those of the azido derivatives. The meso protons of (OEP)In[$N_4C(R)$] have a singlet signal in the range 10.42–10.45 ppm, but this resonance is shifted to lower fields compared to the meso proton signal of (OEP)InN_3. The signals of the methylene protons range between 3.87 and 4.02 ppm, and those of the methyl protons are close to 1.80 ppm. The UV–visible properties of (P)InN_3 and (P)In[$N_4C(R)$] are similar to each other, and similarities also exist in NMR spectra for compounds in the two series. For example, only a small shift of the meso protons to lower fields is observed when N_3^- is replaced by a tetrazolato ligand. Similar spectra are obtained for N_3^- and $N_4C(R)$ complexes in the TPP and Tp-CF_3PP series. This can easily be explained by an anionic character of the tetrazolato group, which appears to be strongest for the three investigated σ-bonded $N_4C(p\text{-}NO_2C_6H_4)$ derivatives.

The coordination schemes of the starting and final products are similar to each other, as shown by the pattern of the methylene protons for the OEP derivatives. The two porphyrin faces are inequivalent, and an ABX_3 coupling is observed for the methylene protons.[38,39] These data agree with pentacoordination of the

(32) Gouterman, M. In *The Porphyrins*; Dolphin, D., Ed.; Academic: New York, 1978; Vol. III, Chapter 1.
(33) Cocolios, P.; Guilard, R.; Fournari, P. *J. Organomet. Chem.* **1979**, *179*, 311.
(34) Kadish, K. M.; Boisselier-Cocolios, B.; Cocolios, P.; Guilard, R. *Inorg. Chem.* **1985**, *24*, 2139.
(35) Nelson, J. H.; Schmitt, D. L.; Henry, R. A.; Moore, D. W.; Jonassen, H. B. *Inorg. Chem.* **1970**, *9*, 2678.
(36) Redfield, D. A.; Nelson, J. H.; Henry, R. A.; Moore, D. W.; Jonassen, H. B. *J. Am. Chem. Soc.* **1974**, *96*, 6298.
(37) Kieft, R. L.; Peterson, W. M.; Blundell, G. L.; Horton, S.; Henry, R. A.; Jonassen, H. B. *Inorg. Chem.* **1976**, *15*, 1721.

Table VI. Infrared Data (ν, cm^{-1}) for the Investigated (P)In[$N_4C(R)$] Complexes (CsI Pellets)

porphyrin, P	axial ligand	ν(R)	$\nu(NO_2)$		ν(tetrazole)						ν(tetrazole) + ν(R)				ν(In–N)
OEP	$N_4C(CH_3)$				1482	1385	1315	1268	1100		805	732	700		298
	$N_4C(CH_2CH_3)$				1480	1410	1312	1267			800				
	$N_4C(C_6H_5)$	3066			1480	1360					785	737	678		305
	$N_4C(p\text{-}NO_2C_6H_4)$		1521	1337		1337	1283	1170			862	733	535	500	290
TPP	$N_4C(CH_3)$				1480	1380		1255			808	760	734	680	
	$N_4C(CH_2CH_3)$					1410		1260	1060	1035			728		
	$N_4C(C_6H_5)$	3070			1490	1365			1070				735	668	
	$N_4C(p\text{-}NO_2C_6H_4)$		1510	1345		1370	1315	1170			855		680	498	285
Tp-CF_3PP	$N_4C(CH_3)$				1435	1380		1230		984			730	702	
	$N_4C(CH_2CH_3)$				1480	1370		1240	1110				725	690	
	$N_4C(C_6H_5)$				1503	1450	1300				880	755	683	632	
	$N_4C(p\text{-}NO_2C_6H_4)$		1520	1350	1485	1445						745	730	690	

Table VII. UV–Visible Data for the Indium(III) Porphyrin Complexes in Tetrahydrofuran

porphyrin, P	axial ligand	λ_{max}, nm ($10^{-3}\epsilon$, M^{-1} cm^{-1})				
		B(1,0)	B(0,0)	Q(2,0)	Q(1,0)	Q(0,0)
OEP	N_3^-	386 (50.6)	408 (314.6)	498 (1.0)	539 (16.4)	577 (17.1)
	$N_4C(CH_3)$	386 (70.4)	407 (483.6)	499 (1.1)	539 (20.0)	577 (22.9)
	$N_4C(CH_2CH_3)$	385 (46.9)	407 (515.6)	499 (1.3)	539 (18.6)	577 (19.7)
	$N_4C(C_6H_5)$	385 (69.7)	407 (460.3)	498 (1.2)	539 (18.4)	576 (20.6)
	$N_4C(p\text{-}NO_2C_6H_4)$	386 (41.8)	407 (407.5)	496 (1.1)	539 (17.4)	576 (18.6)
	$N_3C_2(CO_2CH_3)_2$	386 (35.0)	407 (375.0)	498 (1.4)	541 (18.0)	577 (18.5)
	$N_3C_6H_4$	384 (47.7)	407 (373.8)	504 (1.1)	538 (15.5)	576 (16.8)
TPP	N_3^-	403 (42.7)	425 (561.5)	522 (1.9)	561 (18.5)	601 (9.8)
	$N_4C(CH_3)$	402 (49.0)	424 (596.2)	519 (1.8)	560 (18.0)	600 (7.1)
	$N_4C(CH_2CH_3)$	404 (32.0)	425 (466.7)	522 (3.2)	560 (21.6)	601 (11.1)
	$N_4C(C_6H_5)$	402 (30.9)	425 (394.7)	516 (1.4)	560 (11.9)	600 (5.6)
	$N_4C(p\text{-}NO_2C_6H_4)$	402 (16.0)	425 (662.3)	518 (2.0)	560 (16.8)	600 (9.2)
	$N_3C_2(CO_2CH_3)_2$	403 (32.4)	424 (368.9)	520 (1.6)	561 (11.8)	601 (6.4)
Tp-CF_3PP	N_3^-	404 (48.1)	425 (520.8)	520 (2.5)	560 (20.8)	600 (8.3)
	$N_4C(CH_3)$	402 (50.0)	424 (570.0)	520 (2.2)	560 (20.4)	599 (7.8)
	$N_4C(CH_2CH_3)$	400 (28.5)	422 (540.0)	520 (2.2)	558 (20.1)	598 (7.1)
	$N_4C(C_6H_5)$	402 (46.8)	424 (602.0)	519 (1.8)	559 (20.7)	598 (7.0)
	$N_4C(p\text{-}NO_2C_6H_5)$	402 (31.3)	422 (451.8)	520 (1.3)	560 (15.1)	598 (5.3)
	$N_3C_2(CO_2CH_3)_2$	403 (59.5)	425 (484.8)	518 (1.3)	560 (16.5)	599 (4.6)

indium(III) atom, which should be located above the mean porphyrin plane. The anisotropy of the two macrocyclic faces for complexes in the (TPP)In[$N_4C(R)$] series induces a small chemical shift difference between the two equatorial phenyl ortho protons.

The axial phenyl group protons have either two or three signals in the range 6.41–6.94 ppm, with the ortho protons being the more deshielded. The presence of an $N_4C(p\text{-}NO_2C_6H_4)$ ligand in (P)In[$N_4C(p\text{-}NO_2C_6H_4)$] increases deshielding of the ortho and meta protons, which appear as doublets in the range 6.43–7.22 ppm. The low-field chemical shifts of these protons indicate a large metal–porphyrin plane distance. In addition, the chemical shifts agree with an orbital conjugation between the aryl group and the tetrazole ring.[40] It is therefore likely that the aromatic R group is in the 4-position of the ligand (i.e. isomer II in Chart I). A substitution at the 5-position of the tetrazolato ligand (isomer I) would be sterically hindered, and the axial proton chemical shifts would be at higher fields due to the noncoplanarity of the resulting complex.

The porphyrin macrocycle influences resonances for protons of the alkyl (methyl or ethyl) substituent on the tetrazolato ligand, and either one or two signals shifted upfield from reference are observed. The position of these axial ligand signals will depend upon the nature of the porphyrin macrocycle; the more basic the ring, the more shielded the protons. The order of shielding varies according to the decreasing chemical shifts and is as follows: Tp-CF_3PP < TPP < OEP.

Similar effects are observed for complexes with alkyl and aryl substituents on the tetrazolato ligand, and no correlation is found between the type of isomer formed and the low-field chemical shift of the axial alkyl group. A definitive structure could therefore not be established on the basis of the ^1H NMR results alone, and a crystal structure determination was carried out for one representative compound in each group (i.e. alkyl- and aryltetrazolato ligands) in order to establish the linkage mode of the tetrazolato ligand. These structural data are described in the following section.

Chart III

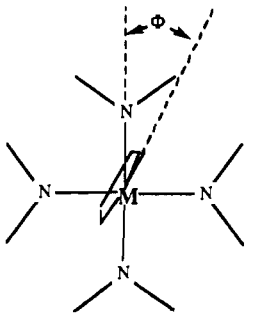

Molecular Structure Description of (OEP)In[$N_4C(C_6H_5)$] (A) and (OEP)In[$N_4C(CH_3)$] (B). Figure 1 presents a view of the two complexes. The phenyl group of complex A is in the 4-position, while the methyl group of complex B is in the 5-position. However, the tetrazolato ligand in both compounds is rigorously planar and tends toward an eclipsed conformation with respect to the two opposite nitrogen atoms of the porphinato core: the ϕ angle, as introduced by Hoard[41] (see Chart III), is 23.9° for A and 8.2° for B. This conformation cannot be explained by steric hindrance considerations alone but can be accounted for by a

(38) Busby, C. A.; Dolphin, D. *J. Magn. Reson.* **1976**, *23*, 211.
(39) Tabard, A.; Guilard, R.; Kadish, K. M. *Inorg. Chem.* **1986**, *25*, 4277.
(40) Takach, N. E.; Holt, E. M.; Alcock, N. W.; Henry, R. A.; Nelson, J. H. *J Am. Chem. Soc.* **1980**, *102*, 2968.
(41) Collins, D. M.; Countryman, R.; Hoard, J. L. *J. Am. Chem. Soc.* **1972**, *94*, 2066.

Table VIII. ^{1}H NMR Data[a] for (P)InN$_3$ and (P)In[N$_4$C(R)] where R = CH_3, CH_2CH_3, C_6H_5, p-$NO_2C_6H_4$

porphyrin, P	axial ligand	R^1	R^2	protons of R^1	multi/intens	δ	protons of R^2	multi/intens	δ	protons of R	multi/intens	δ
OEP	N_3^-	H	CH_2CH_3	meso H	s/4	+10.39	α-CH_2	m/8	+4.01			
							α'-CH_2	m/8	+3.90			
							β-CH_3	t/12	+1.82			
	$N_4C(CH_3)$	H	CH_2CH_3	meso H	s/4	+10.42	α-CH_2	m/8	+4.00	CH_3	s/3	−0.38
							α'-CH_2	m/8	+3.88			
							β-CH_3	t/12	+1.78			
	$N_4C(CH_2CH_3)$	H	CH_2CH_3	meso H	s/4	+10.42	α-CH_2	m/8	+4.00	CH_3	t/3	−0.49
							α'-CH_2	m/8	+3.88	CH_2	q/2	−0.20
							β-CH_3	t/12	+1.79			
	$N_4C(C_6H_5)$	H	CH_2CH_3	meso H	s/4	+10.42	α-CH_2	m/8	+4.02	ortho H	d/2	+6.68
							α'-CH_2	m/8	+3.87	para H	t/1	+6.46
							β-CH_3	t/12	+1.80	meta H	t/2	+6.41
	$N_4C(p$-$NO_2C_6H_4)$	H	CH_2CH_3	meso H	s/4	+10.45	α-CH_2	m/8	+4.02	ortho H	d/2	+7.06
							α'-CH_2	m/8	+3.87	meta H	d/2	+6.43
							β-CH_3	t/12	+1.80			
TPP	N_3^-	C_6H_5	H	ortho H	m/8	+8.05	pyrrole H	s/8	+9.04			
				meta, para H	m/12	+7.47						
	$N_4C(CH_3)$	C_6H_5	H	ortho H	m/8	+8.03	pyrrole H	s/8	+9.09	CH_3	s/3	−0.33
				meta, para H	m/12	+7.44						
	$N_4C(CH_2CH_3)$	C_6H_5	H	ortho H	m/8	+8.04	pyrrole H	s/8	+9.04	CH_3	t/3	−0.36
				meta, para H	m/12	+7.45				CH_2	q/2	−0.01
	$N_4C(C_6H_5)$	C_6H_5	H	ortho H	m/8	+8.02	pyrrole H	s/8	+9.04	ortho H	m/2	+6.87
				meta, para H	m/12	+7.45				meta, para H	m/3	+6.56
	$N_4C(p$-$NO_2C_6H_4)$	C_6H_5	H	ortho H	m/8	+8.06	pyrrole H	s/8	+9.06	ortho H	d/2	+7.20
				meta, para H	m/12	+7.46				meta H	d/2	+6.75
Tp-CF_3PP	N_3^-	p-$CF_3C_6H_4$	H	ortho H	d/4	+7.88	pyrrole H	s/8	+8.86			
				ortho′ H	d/4	+7.87						
				meta H	d/4	+7.70						
				meta′ H	d/4	+7.67						
	$N_4C(CH_3)$	p-$CF_3C_6H_4$	H	ortho H	d/4	+7.89	pyrrole H	s/8	+8.87	CH_3	s/3	−0.32
				ortho′ H	d/4	+7.87						
				meta H	d/4	+7.69						
				meta′ H	d/4	+7.65						
	$N_4C(CH_2CH_3)$[b]	p-$CF_3C_6H_4$	H	ortho H	d/4	+7.83	pyrrole H	s/8	+8.83	CH_2CH_3	m/5	−0.21
				ortho′ H	d/4	+7.79						
				meta H	d/4	+7.70						
				meta′ H	d/4	+7.68						
	$N_4C(C_6H_5)$	p-$CF_3C_6H_4$	H	ortho H	d/4	+7.92	pyrrole H	s/8	+8.88	ortho H	d/2	+6.94
				ortho′ H	d/4	+7.86				meta, para H	m/3	+6.58
				meta H	d/4	+7.72						
				meta′ H	d/4	+7.66						
	$N_4C(p$-$NO_2C_6H_4)$	p-$CF_3C_6H_4$	H	ortho H	d/4	+7.90	pyrrole H	s/8	+8.88	ortho H	d/2	+7.22
				ortho′ H	d/4	+7.88				meta H	d/2	+6.81
				meta H	d/4	+7.72						
				meta′ H	d/4	+7.68						

[a] Spectra were recorded in C_6D_6 at 21 °C with $SiMe_4$ as internal reference; chemical shifts downfield from $SiMe_4$ are defined as positive. Key: R^1 = porphyrin methine group; R^2 = porphyrin pyrrole group; R = substituent of axial tetrazolato group; s = singlet; d = doublet; t = triplet; q = quadruplet; m = multiplet. [b] δ (ppm) in $CDCl_3$ (at 21 °C): 8.45 (4 H, d, ortho H(R^1)), 8.28 (4 H, d, ortho H(R^1)), 8.12 (4 H, d, meta H(R^1)), 8.08 (4 H, d, meta′ H(R^1)), 9.10 (8 H, s, pyrrole H), −0.54 (3 H, t, CH_3(R)), −0.66 (2 H, q, CH_2(R)).

pπ–pπ interaction, as discussed for the analogous Fe(III) σ-bonded complexes, (OEP)Fe[N$_4$C(C_6H_5)] and (OEP)Fe[N$_4$C(CH_3)].[9]

A comparison of bond distances and angles for the tetrazolato groups of (OEP)Fe[N$_4$C(C_6H_5)] and (OEP)Fe[N$_4$C(CH_3)] is difficult because the linkage modes are different in each of the two complexes. However, it appears that the bond distances are equal within 0.03 Å for A while in B the C41–N6 and N8–N7 bonds (1.28 (2) and 1.29 (1) Å, respectively) seem to have a more pronounced double-bond character (see Figure 2). The dihedral angle between the phenyl group and the tetrazole ring of (OEP)In[N$_4$C(C_6H_5)] is 11.6°, favoring orbital conjugation between the two cycles. This was also observed in the ^{1}H NMR data and would explain the short C41–C42 bond (1.45 (1) Å) between the phenyl and tetrazole rings. The differences between the two substituents do not influence the stereochemical parameters of the indium coordination polyhedron. The In–N(P) and In–N(5) bond lengths and the distance of the indium atom from the porphyrin plane are almost the same (Δ4N(A) = 0.463 Å, Δ4N(B) = 0.499 Å) (see also Table V). The doming character is very small in (OEP)In[N$_4$C(C_6H_5)] (0.03 Å) compared to that of (OEP)Fe[N$_4$C(CH_3)] (0.12 Å).

Table IX lists the available crystal structure data for different group 13 metalloporphyrins (M = Al, Ga, In, Tl). As shown in this table, the Δ4N and ΔP parameters depend upon the axial ligand. The value of Δ4N varies from 0.463 to 0.791 Å for indium porphyrins and from 0.617 to 1.000 Å for thallium porphyrins. The complexes with alkyl ligands have almost the same parameters as those with metalate ligands. This might be expected since both sets of σ-bonded ligands pull the metal out of plane. In contrast, the two complexes with ionic tetrazolato ligands push the metal into the plane of the four nitrogens.[42]

(42) Guilard, R.; Lecomte, C.; Kadish, K. M. *Struct. Bonding* **1987**, *64*, 205.
(43) Guilard, R.; Zrineh, A.; Tabard, A.; Endo, A.; Han, B. C.; Lecomte, C.; Souhassou, M.; Habbou, A.; Ferhat, M.; Kadish, K. M. *Inorg. Chem.* **1990**, *29*, 4476.

Table IX. Stereochemical Parameters[a] for Group 13 Pentacoordinated Porphyrin Complexes

compd	distance, Å				ref
	M–N(P)	M–L	Δ4N	ΔP	
(OEP)Al(CH_3)	2.030	1.936	0.470	0.530	43
(OEP)Ga(SO_3CH_3)	2.010	1.908 (6)	0.320	0.329	44
(OEP)GaN_3	2.030	1.955 (2)	0.362	0.398	45
(TPP)GaCl	2.020	2.196 (2)	0.317	0.317	46
(TPP)InCl	2.160	2.369 (2)	0.610	0.710	47
(TPP)In(CH_3)	2.200	2.13 (1)	0.780	0.920	48
(OEP)In[$N_4C(C_6H_5)$]	2.130	2.183 (5)	0.463	0.494	7 and this work
(OEP)In[$N_4C(CH_3)$]	2.140	2.181 (5)	0.490	0.490	this work
(OEP)In[$Mn(CO)_5$]	2.190	2.705 (1)	0.744	0.814	49
(OEP)In[$Mo(CO)_3Cp$]	2.200	2.890 (1)	0.791	0.860	50
(OEP)TlCl	2.210	2.449 (3)	0.690	0.750	51
(TPP)TlCl	2.210	2.420 (4)	0.617	0.737	51
(TPP)Tl(CH_3)	2.290	2.15 (1)	0.839	0.979	52
(TPP)Tl(NOR)	2.290	2.09 (1)	0.900	1.100	53
(OEP)Tl[$Mn(CO)_5$]	2.260	2.649 (1)	0.939	0.975	54
(OEP)Tl[$Mo(CO)_3Cp$]	2.290	2.829 (5)	1.000	1.060	55

[a] Abbreviations: Cp = cyclopentadienyl; NOR = 2-*exo*-3-*exo*-(carboxylatomethyl)-bicyclo[2.2.1]hept-5-enyl; M–N(P) = average distance from the metal ion to a pyrrole nitrogen; M–L = metal–axial ligand bond distance; Δ4N = distance from the plane of the four nitrogen atoms to the metal center; ΔP = distance from the mean plane of the $C_{20}N_4$ porphinato core atoms to the metal ion.

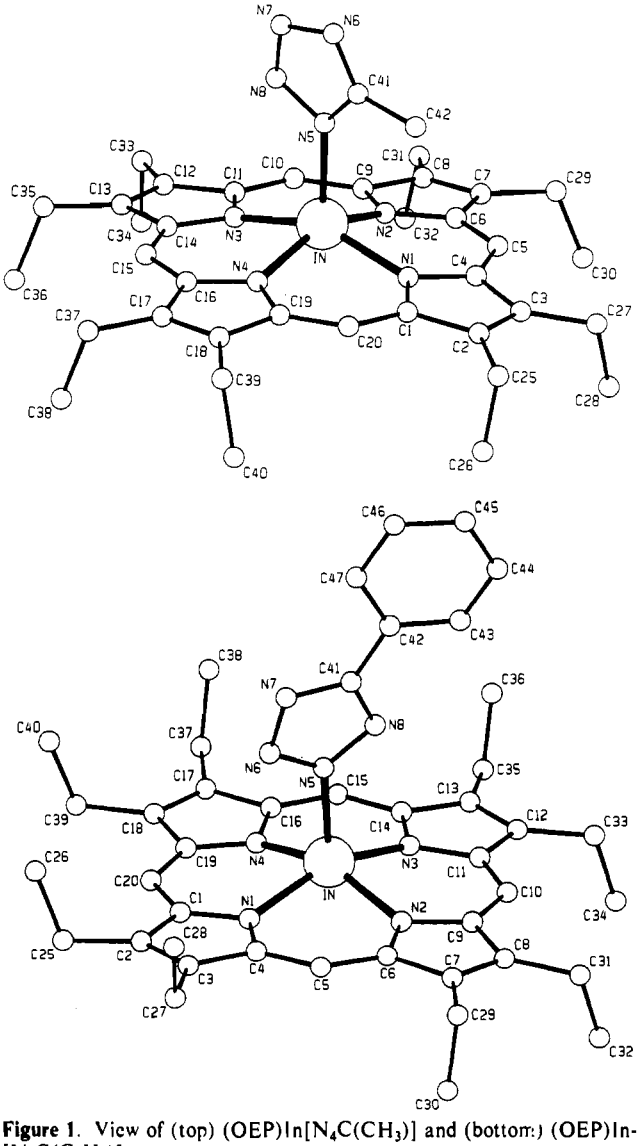

Figure 1. View of (top) (OEP)In[$N_4C(CH_3)$] and (bottom) (OEP)In[$N_4C(C_6H_5)$].

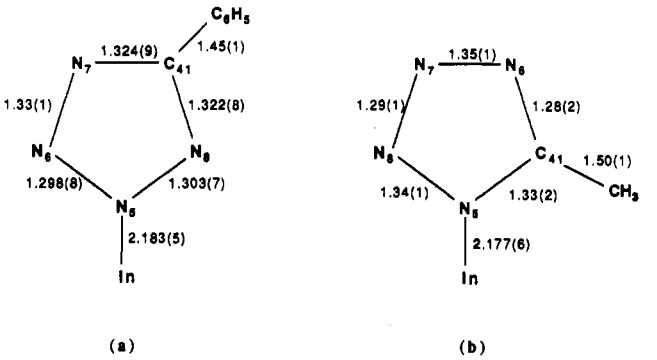

Figure 2. Main bond lengths and angles in the tetrazolato group of (a) (OEP)In[$N_4C(C_6H_5)$] and (b) (OEP)In[$N_4C(CH_3)$].

Characterization of Neutral (P)In[$N_3C_2(CO_2CH_3)_2$] and (OEP)In($N_3C_6H_4$) Complexes. The reaction of dimethyl acetylenedicarboxylate with organic[2-5] and organometallic[12,19,56,57] azides is well-known, but to our knowledge, studies concerning the reactivity of metal azido complexes with benzyne have yet to be described in the literature.

The reactions of (P)InN_3 with dimethyl acetylenedicarboxylate (P = OEP, TPP, and Tp-CF_3PP) or benzyne (P = OEP) were both investigated in this present study. The analytical data for the resulting compounds are summarized in Table I and indicate the formation of a metalloporphyrin with an axially complexed triazole ring. As already reported,[58] the reactivity of (OEP)InN_3

(44) Boukhris, A.; Lecomte, C.; Coutsolelos, A.; Guilard, R. *J. Organomet. Chem.* **1986**, *303*, 151.
(45) Coutsolelos, A. Guilard, R.; Boukhris, A.; Lecomte, C. *J. Chem. Soc., Dalton Trans.* **1986**, 1779.
(46) Coutsolelos, A.; Guilard, R.; Bayeul, D.; Lecomte, C. *Polyhedron* **1986**, *5*, 1157.
(47) Ball, R. G.; Lee, K. M.; Marshall, A. G.; Trotter, J. *Inorg. Chem.* **1980**, *19*, 1463.
(48) Lecomte, C.; Protas, J.; Cocolios, P.; Guilard, R. *Acta Crystallogr.* **1980**, *B36*, 2769.
(49) Guilard, R.; Mitaine, P.; Moïse, C.; Lecomte, C.; Boukhris, A.; Swistak, C.; Tabard, A.; Lacombe, D.; Cornillon, J.-L.; Kadish, K. M. *Inorg. Chem.* **1987**, *26*, 2467.
(50) Lecomte, C.; Habbou, A.; Mitaine, P.; Richard; P.; Guilard, R. *Acta Crystallogr.* **1989**, *C45*, 1226.
(51) Cullen, D. L.; Meyer, E. F.; Smith, K. M. *Inorg. Chem.* **1977**, *16*, 1179.
(52) Henrick, K.; Matthews, R. W.; Tasker, P. A. *Inorg. Chem.* **1977**, *16*, 3293.
(53) Brady, F.; Henrick, K.; Matthews, R. W. *J. Organomet. Chem.* **1981**, *210*, 281.
(54) Guilard, R.; Zrineh, A.; Ferhat, M.; Tabard, A.; Mitaine, P.; Swistak, C.; Richard, P.; Lecomte, C.; Kadish, K. M. *Inorg. Chem.* **1988**, *27*, 697.
(55) Richard, P.; Zrineh, A.; Guilard, R.; Habbou, A.; Lecomte, C. *Acta Crystallogr.* **1989**, *C45*, 1224.
(56) Hsieh, B.-T.; Takach, N. E.; Milosavljevic, E. B.; Nelson, J. H.; Kemmerich, T.; Beck, W.; Bresciani-Pahor, N.; Randaccio, L.; Brower, K. R. *Inorg. Chim. Acta* **1987**, *134*, 31.
(57) Hsieh, B.-T.; Nelson, J. H.; Milosavljevic, E. B.; Beck, W.; Kemmerich, T. *Inorg. Chim. Acta* **1987**, *133*, 267.

Table X. Infrared Data (ν, cm^{-1}) for the Investigated Triazolato Complexes (CsI Pellets)

porphyrin, P	axial ligand	ν(C=O)	ν(C-O)	ν(C-H)		triazole ring vibrations							
OEP	$N_3C_2(CO_2CH_3)_2$	1730	1228			1510	1445	1195	1175	1090	820	770	
	$N_3C_6H_4$						1485	1240				672	
TPP	$N_3C_2(CO_2CH_3)_2$	1730	1225	2950	2920	1510	1432	1395	1320	1290	1087	820	770
Tp-CF_3PP	$N_3C_2(CO_2CH_3)_2$	1735	1220	2950		1505					1085		

Table XI. ^{1}H NMR Data[a] for the Triazolato Complexes

porphyrin, P	axial ligand	R^1	R^2	protons of R^1	multi/intens	δ	protons of R^2	multi/intens	δ	protons of axial ligand	multi/intens	δ
OEP	$N_3C_2(CO_2CH_3)_2$	H	CH_2CH_3	meso H	s/4	+10.41	α-CH_2	m/8	+4.02	CH_3	s/6	+2.57
							α'-CH_2	m/8	+3.86			
							β-CH_3	t/24	+1.80			
	$N_3C_6H_4$	H	CH_2CH_3	meso H	s/4	+10.47	α-CH_2	m/8	+4.06		t/1	+5.89
							α'-CH_2	m/8	+3.94		br/1	+5.69
							β-CH_3	t/24	+1.86		d/1	+5.61
											t/1	+5.43
TPP	$N_3C_2(CO_2CH_3)_2$	C_6H_5	H	ortho H	d/4	+8.18	pyrrole H	s/8	+9.05	CH_3	s/6	+2.71
				ortho' H	d/4	+8.08						
				meta, para H	m/12	+7.48						
Tp-CF_3PP	$N_3C_2(CO_2CH_3)_2$	*p*-$CF_3C_6H_4$	H	ortho H	d/4	+8.03	pyrrole H	s/8	+8.88	CH_3	s/6	+2.67
				ortho' H	d/4	+7.93						
				meta H	d/4	+7.71						
				meta' H	d/4	+7.67						

[a] Spectra were recorded in C_6D_6 at 294 K with $SiMe_4$ as internal reference; chemical shifts downfield from $SiMe_4$ are defined as positive. Key: R^1 = porphyrin methine group; R^2 = porphyrin pyrrole group; s = singlet; d = doublet; t = triplet; m = multiplet; br = broad peak.

toward an organic acid is poor compared to the same reaction of (TPP)InN_3. For this reason, all attempts to synthesize the benzotriazolato tetraphenylporphyrin or benzotriazolato tetrakis(*p*-(trifluoromethyl)phenyl)porphyrin compounds were unsuccessful and only the carboxylato compounds could be isolated.

The yields of the tetrazolato complexes do not appear to depend upon the nature of the porphyrin macrocycle, but this is not the case for the triazolato complexes. The highest yield (69%) is obtained for (OEP)In[$N_3C_2(CO_2CH_3)_2$], while the lowest (47%) is obtained for (Tp-CF_3PP)In[($N_3C_2(CO_2CH_3)_2$]. These differences cannot be explained by the reactivity of the dipolarophile or the polarophile, but the formation of different kinetic or thermodynamic products might be invoked.

Table X summarizes IR vibration frequencies of the triazolato complexes in the solid state. As expected, an N_3^- vibration is not observed after completion of the reaction. When the dipolarophile is dimethyl acetylenedicarboxylate, the resulting product has two absorptions characteristic of C=O and C—O groups. These occur in the ranges 1730–1735 and 1220–1228 cm^{-1} (see Table X). Bands close to 2900 cm^{-1} are attributed to the methyl group of (P)In[$N_3C_2(CO_2CH_3)_2$], while vibrations in the range 672–1510 cm^{-1} confirm the presence of a linked triazole ring.[12]

The presence of only one carbonyl absorption in the infrared spectrum of (P)In[$N_3C_2(CO_2CH_3)_2$] indicates that a thermodynamic product of the type shown in Chart IIa is formed. The vibrations of (OEP)In($N_3C_6H_4$) are weak, and only three bands attributed to the axial-bound triazolato ligand are observed.

UV–visible spectra of the triazolato complexes are similar to those of both the tetrazolato complexes and the starting azido derivatives. This shows that reaction of a dipolarophile with axially complexed N_3^- does not significantly modify the electronic level of the porphyrin product with respect to the starting compound. Moreover, the UV–visible absorptions do not substantially vary with the type of isomer, as was already described for the tetrazolato complexes. This indicates that the energy gap between the kinetic and thermodynamic products is small and that a determination of other axial ligand physicochemical characteristics is needed in order to definitively elucidate the type of isomer.[35] One such characteristic, which should establish the structures of the investigated triazolato complexes, is ^{1}H NMR spectroscopy.

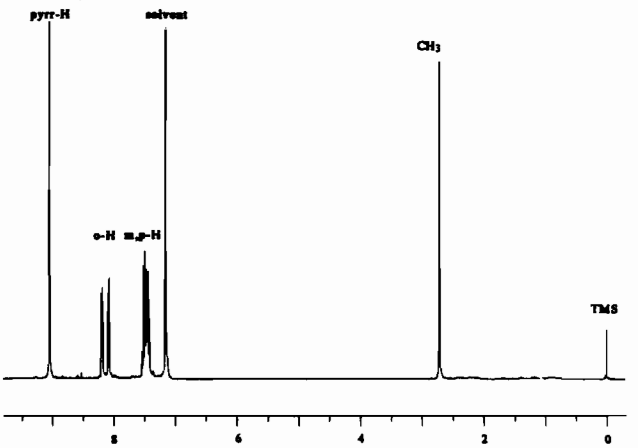

Figure 3. ^{1}H NMR spectrum of (TPP)In[$N_3C_2(CO_2CH_3)_2$] recorded at 21 °C in C_6D_6.

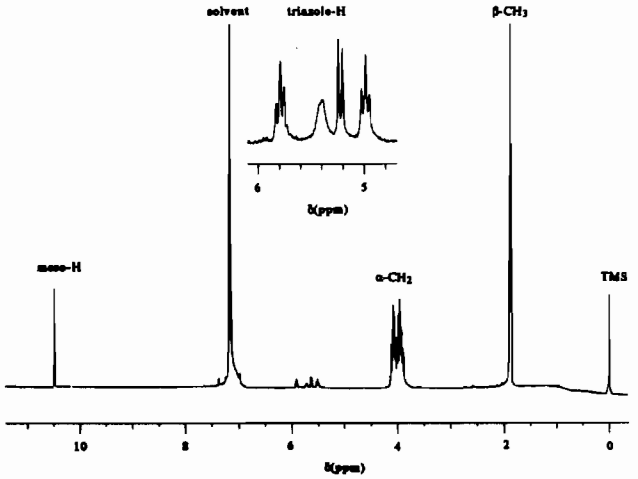

Figure 4. ^{1}H NMR spectrum of (OEP)In($N_3C_6H_4$) recorded at 21 °C in C_6D_6.

A summary of the ^{1}H NMR data for the four synthesized triazolato complexes is given in Table XI. Methyl protons for the bound bis(methylcarboxylato)triazolato ligand appear as a singlet between 2.57 and 2.71 ppm in C_6D_6 (see Figure 3). The

(58) Cocolios, P.; Guilard, R.; Bayeul, D.; Lecomte, C. *Inorg. Chem.* **1985**, *24*, 2058.

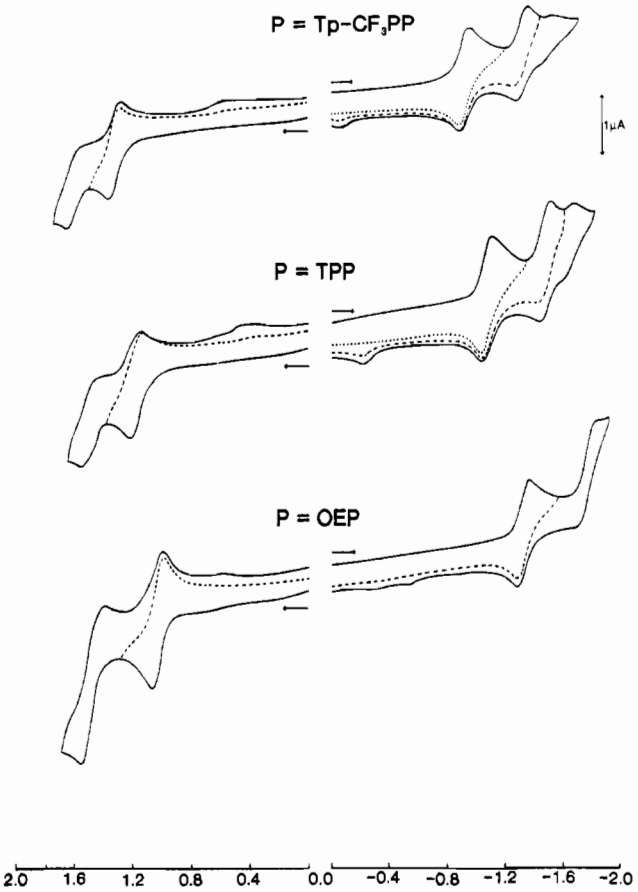

Figure 5. Cyclic voltammograms for the reduction and oxidation of three (P)In[$N_4C(C_6H_5)$] complexes in CH_2Cl_2, 0.1 M (TBA)ClO_4. Scan rate = 0.1 V/s.

position of the proton resonance indicates a small shielding compared to the signal of either dimethyl acetylenedicarboxylate (3.02 ppm) or a noncoordinated triazolate ion (3.39 ppm) in C_6D_6. Significant changes in the methyl proton resonances do not occur with changes in the nature of the macrocycle. This indicates that the distance of the methyl protons from the porphyrin plane is large, and this result is consistent with a thermodynamic product (see Chart IIa). The four protons of the benzotriazolato derivative have four signals in the range 5.43–5.89 ppm (see Table XI and Figure 4), which results from an inequivalence of the four protons. This demonstrates that the addition of benzyne to a coordinated azido group leads to a kinetic product, as shown in Chart IIb, and also suggests that steric hindrance is the main driving force in determining the resulting kinetic or thermodynamic product.

Electrochemistry. Typical cyclic voltammograms of (Tp-CF_3PP)In[$N_4C(C_6H_5)$], (TPP)In[$N_4C(C_6H_5)$], and (OEP)In-[$N_4C(C_6H_5)$] in CH_2Cl_2 are represented in Figure 5, and half-wave potentials for the oxidation and reduction of each tetrazolato or triazolato complex in CH_2Cl_2 are listed in Table XII. The potential difference between the first reduction and the first oxidation varies between 2.17 and 2.33 V and is largest for the OEP complexes. The difference in $E_{1/2}$ between the first and second reduction is 0.37–0.47 V, while that between the first and second oxidation ranges between 0.28 and 0.46 V. These data all indicate that each electron transfer most likely occurs at the porphyrin π ring system.[59,60] As expected, there is a negative shift of the half-wave potentials that follows the trend Tp-CF_3PP > TPP > OEP.

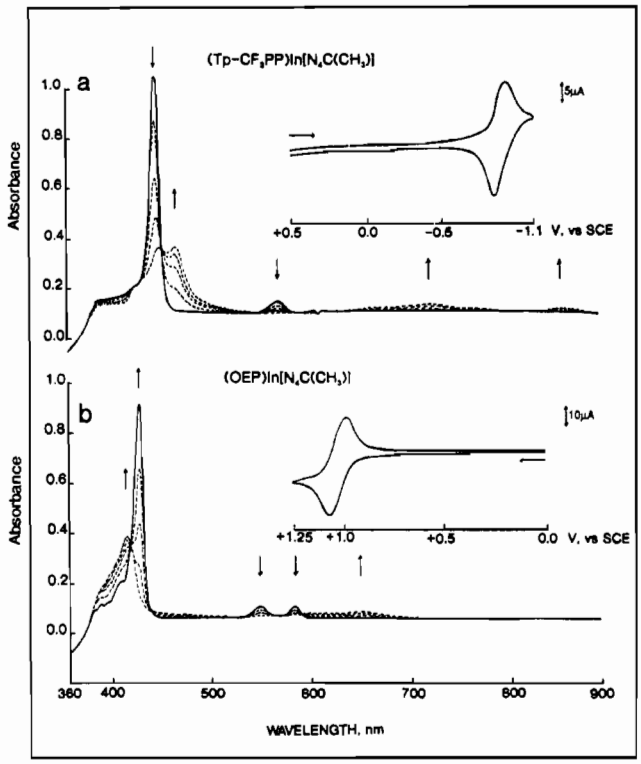

Figure 6. Time-resolved thin-layer electronic absorption spectra and thin-layer cyclic voltammograms for (a) first reduction of (Tp-CF_3PP)-In[$N_4C(CH_3)$] and (b) the first oxidation of (OEP)In[$N_4C(CH_3)$] in CH_2Cl_2, 0.1 M (TBA)ClO_4.

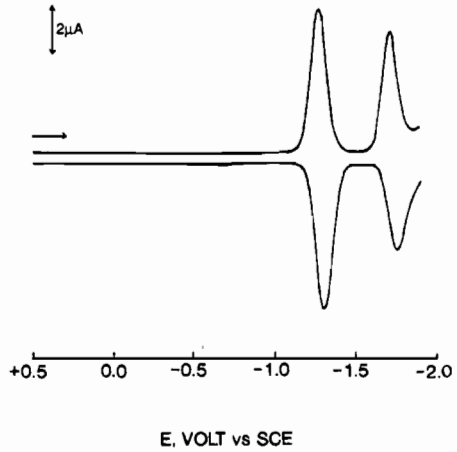

Figure 7. Differential pulse voltammogram of (OEP)In[$N_4C(CH_3)$] in CH_2Cl_2, 0.1 M (TBA)ClO_4.

Thin-layer cyclic voltammograms and the resulting thin-layer spectra after the first reduction of (Tp-CF_3PP)In[$N_4C(CH_3)$] or the first oxidation of (OEP)In[$N_4C(CH_3)$] are shown in Figure 6. Both electron transfers are reversible and agree with data from differential pulse voltammetry under the same solution conditions (see Figure 7).

The transfer of a single electron in the reduction of (Tp-CF_3PP)In[$N_4C(C_6H_5)$] was demonstrated by controlled-potential coulometry at −1.20 V and gave $n = 0.91 \pm 0.10$. The second reduction occurs at $E_{1/2} = -1.31$ V and is also reversible (see Figure 5). However, a third reduction peak with reduced current intensity appears at $E_{1/2} = -1.50$ V while a similar third peak is located at $E_{1/2} = -1.64$ V for (TPP)In[$N_4C(C_6H_5)$]. A third process is not observed for (OEP)In[$N_4C(C_6H_5)$] but is present for all of the other TPP or Tp-CF_3PP derivatives after scanning to potentials negative of the second reduction. Also, when the potential scan is reversed at potentials beyond the second reduction, a small oxidation peak appears on the reverse scan. This peak is present for most of the complexes and is shown in Figure 5 for

(59) Fuhrhop, J.-H.; Kadish, K. M.; Davis, D. G. *J. Am. Chem. Soc.* **1973**, *95*, 5140.
(60) Felton, R. H. In *The Porphyrins*; Dolphin, D., Ed.; Academic: New York, 1978; Vol. V, Chapter 3 (see also references therein).

Table XII. Half-Wave Potentials (V vs SCE) of the Investigated Tetrazolato and Triazolato Complexes in CH_2Cl_2 Containing 0.1 M (TBA)ClO_4 (Scan Rate = 100 mV/s)

porphyrin, P	axial ligand	oxidation			reduction			$\lvert E_{1/2}$(oxidn) − $E_{1/2}$(redn)$\rvert$[f]
		1st	2nd	$\Delta E_{1/2}$	1st	2nd	$\Delta E_{1/2}$	
OEP	$N_4C(CH_3)$	1.01	1.46	0.45	−1.30	−1.75	0.45	2.31
	$N_4C(CH_2CH_3)$	1.06	1.44	0.38	−1.25	−1.72	0.47	2.31
	$N_4C(C_6H_5)$	1.03	1.49	0.46	−1.30	−1.74	0.44	2.33
	$N_4C(p\text{-}NO_2C_6H_4)$	1.07			[c]	[c]		
	$N_3C_2(CO_2CH_3)_2$	1.04	[d]		−1.28	−1.74	0.46	2.32
TPP	$N_4C(CH_3)$	1.06	1.49	0.43	−1.02[a]	−1.49		
	$N_4C(CH_2CH_3)$	1.17	1.47	0.30	−1.00	−1.42	0.42	2.17
	$N_4C(C_6H_5)$	1.17	1.51	0.34	−1.08	−1.47	0.39	2.25
	$N_3C_2(CO_2CH_3)_2$[b]	1.22	1.50	0.28	−1.02	−1.43	0.41	2.24
Tp-CF_3PP	$N_4C(CH_3)$	1.32	1.60	0.28	−0.89	−1.26	0.37	2.21
	$N_4C(C_6H_5)$	1.32	1.62	0.30	−0.91	−1.31	0.40	2.23
	$N_4C(p\text{-}NO_2C_6H_4)$	1.28	1.64	0.36	[e]	[e]		
	$N_3C_2(CO_2CH_3)_2$	1.31	1.65	0.34	−0.87	−1.27	0.40	2.18

[a] E_p measured at a scan rate of 100 mV/s. [b] Compound has extra peaks at $E_{1/2}$ = 1.16 V and E_{pc} = −0.88 V. [c] Two reductions of the p-$NO_2C_6H_4$ group occur in addition to the porphyrin-ring-centered reactions. The overall electrode reactions are located at E_{pc} = −0.83 V and $E_{1/2}$ = −1.11 and −1.31 V for a scan rate of 100 mV/s. [d] Irreversible oxidation due to coupled chemical reaction(s). [e] Four reactions are observed at E_p = −0.80 V and $E_{1/2}$ = −0.94, −1.11, and −1.31 V. [f] Absolute difference between $E_{1/2}$ for the first oxidation and the first reduction.

Table XIII. Peak Maximum Wavelengths and Molar Absorptivities of (P)In[N_4C(R)] Complexes in CH_2Cl_2, 0.2 M (TBA)PF_6

porphyrin, P	axial ligand	electrode reacn	λ_{max}, nm($10^{-3}\epsilon$, M^{-1} cm^{-1})			
			Soret region		Q bands	
OEP	$N_4C(CH_3)$	none	386 (71)	406 (436)	538 (20)	575 (21)
		1st redn	409 (105)	446 (82)	631 (14)	805 (17)
		1st oxidn		392 (156)	648 (16)	
	$N_4C(C_6H_5)$	none	386 (81)	406 (508)	538 (24)	576 (23)
		1st redn	407 (127)	446 (195)	631 (30)	808 (34)
		1st oxidn		391 (205)	648 (22)	
TPP	$N_4C(CH_3)$	none	404 (40)	424 (376)	559 (17)	598 (8)
		1st redn	426 (124)	447 (101)	730 (15)	861 (8)
		1st oxidn	418 (115)	457 (32)		
	$N_4C(C_6H_5)$	none	403 (37)	424 (380)	559 (14)	598 (6)
		1st redn	425 (177)	448 (68)	731 (10)	861 (6)
		1st oxidn	419 (166)	479 (28)		
Tp-CF_3PP	$N_4C(CH_3)$	none	402 (46)	422 (573)	557 (24)	595 (8)
		1st redn	427 (175)	444 (175)	724 (20)	867 (8)
		1st oxidn	410 (154)	438 (94)	693 (9)	889 (10)
	$N_4C(C_6H_5)$	none	402 (58)	423 (545)	558 (23)	596 (7)
		1st redn	426 (24)	445 (121)	725 (14)	865 (10)
		1st oxidn	410 (186)	478 (45)		

the case of (TPP)In[$N_4C(C_6H_5)$], where E_p is located at −0.22 V.

The third reduction of (P)In[$N_4C(C_6H_5)$] is due to a species generated by a chemical reaction involving the porphyrin anion radical or dianion and disappears at high-potential scan rate. This is demonstrated in Figure 8, which illustrates cyclic voltammograms for the reduction of (Tp-CF_3PP)In[$N_4C(C_6H_5)$] in CH_2Cl_2, 0.1 M (TBA)ClO_4. As seen in this figure, the currents due to the third peak decrease in intensity as the scan rate is increased and totally disappear at a potential scan rate of 1000 mV/s.

Spectral Characterization of Oxidized and Reduced (P)In[N_4C(R)]. Time-resolved electronic absorption spectra were recorded in a thin-layer cell during the first reduction and the first oxidation of each tetrazolato complex (see Table XIII). The spectrum of (Tp-CF_3PP)In[$N_4C(CH_3)$] in CH_2Cl_2, 0.1 M (TBA)ClO_4 exhibits a Soret band at 422 nm and two Q bands at 557 and 595 nm (see Figure 6a). The Soret band is red-shifted by 22 nm upon reduction by one electron. At the same time, the two Q bands disappear and two broad bands appear at 724 and 867 nm. These new peaks are both characteristic of porphyrin π anion radicals.[61] There are no intermediate species formed in the reduction, as suggested by the presence of isosbestic points as 430, 550, and 572 nm. Also, a spectrum identical with that of the starting species is obtained after back-electrolysis at a controlled potential of 0.0 V.

Figure 6b shows the evolution of the UV–visible spectrum during controlled-potential oxidation of (OEP)In[$N_4C(CH_3)$] at +1.2 V. As the electrolysis proceeds, the Soret band blue-shifts from 406 to 392 nm, while the bands at 538 and 575 nm decrease in intensity and finally disappear. At the same time, a broad band characteristic of a porphyrin π cation radical[61,62] appears at 648 nm. The oxidized species is stable with time, and the intial spectrum could be regenerated by back-electrolysis.

Spectral changes upon oxidation or reduction of the other complexes are similar to those described above (see Table XIII) and the final in UV–visible spectra are all typical of porphyrin π anion or π cation radicals. For compounds in a given porphyrin series (OEP, TPP, or Tp-CF_3PP), the final spectra are essentially independent of the bound axial ligand.

An ESR spectrum of the species obtained at low temperature after bulk controlled-potential electrolysis of (OEP)In[$N_4C(C_6H_5)$] in CH_2Cl_2 at −1.5 V is shown in Figure 9. The g factor is close to the free spin value of 2.003, and the shape of the ESR spectrum is similar to the one obtained for reduced (TPP)InClO_4.[61] Although the total width of the signal is close to 180 G, the width between points of the maximum slope is close to 18 G. The value of 180 G is similar to the one value observed in the broad signal reported by Fajer et al.[63] for a zinc porphyrin radical anion. This curve shape appears to result from some poorly resolved spectrum

(61) Kadish, K. M.; Cornillon, J.-L.; Cocolios, P.; Tabard, A.; Guilard, R. *Inorg. Chem.* **1985**, *24*, 3645.
(62) Felton, R. H.; Linschitz, H. *J. Am. Chem. Soc.* **1966**, *88*, 1113.
(63) Fajer, J.; Borg, D. C.; Forman, A.; Felton, R. H.; Vegh, C.; Dolphin, D. *Ann. N.Y. Acad. Sci.* **1973**, *206*, 349.

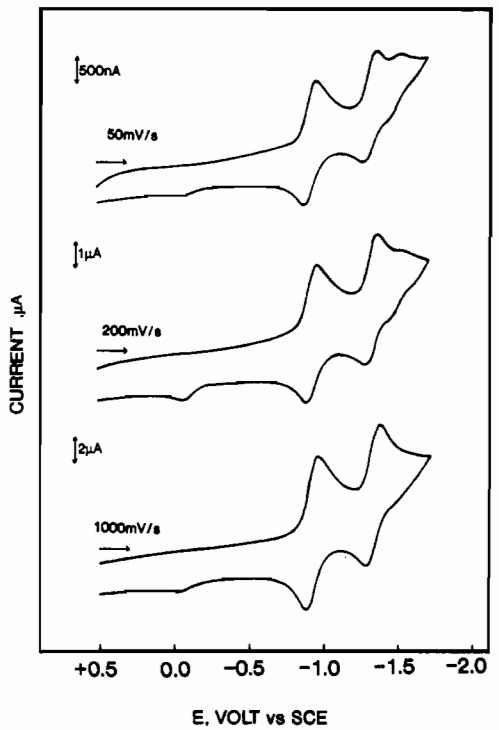

Figure 8. Cyclic voltammograms for the reduction of (Tp-CF_3PP)In-[$N_4C(C_6H_5)$] in CH_2Cl_2, 0.1 M (TBA)ClO_4 at scan rates of 50, 200, and 1000 mV/s.

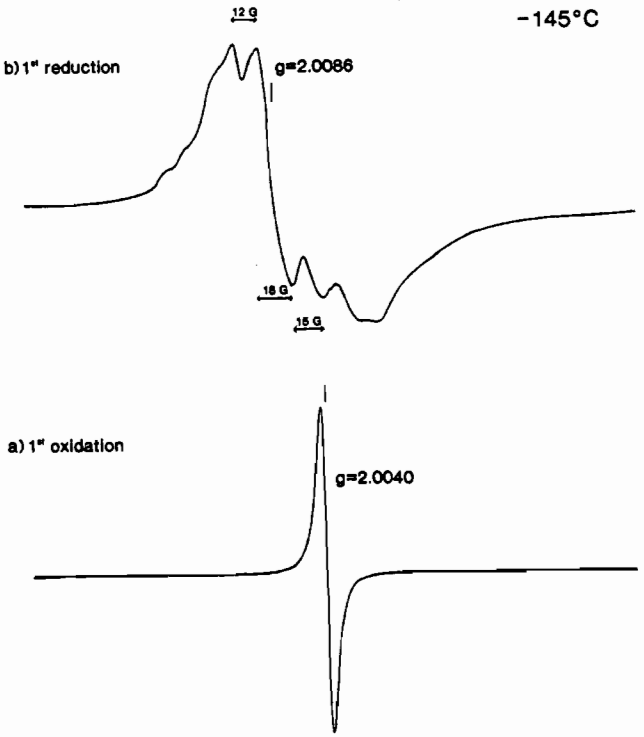

Figure 9. ESR spectra of (a) singly oxidized (OEP)In[$N_4C(C_6H_5)$] and (b) singly reduced (OEP)In[$N_4C(C_6H_5)$] at −145 °C in CH_2Cl_2, 0.1 M (TBA)ClO_4.

of hyperfine structure, which is due to a small interaction of the unpaired electron with the nuclear spin of indium ($I = {}^9/_2$), and also indicates a contribution of protons from the macrocycle, as was shown to be the case for zinc porphyrins.[61] It was not possible to record an ESR signal of the singly reduced species at room temperature, since this signal disappears above 160 K. However, the same ESR spectrum reappears upon repeatedly raising and then lowering the temperature.

The ESR spectrum of electrooxidized (OEP)In[$N_4C(C_6H_5)$] has a very narrow signal centered at $g = 2.004$. The signal is similar at room and low temperature, the latter of which is illustrated in Figure 9. The unpaired electron of the cation radical is largely delocalized on the macrocycle, and little interaction occurs with the metal center.

Table XIV. Half-Wave Potentials for the First Reduction of (TPP)InX and (TPP)In(R) Complexes and Ratios of the Q Band Molar Absorptivities

no.	axial ligand	$E_{1/2}$, V vs SCE	$\epsilon(\alpha)/\epsilon(\beta)$	ref
1	$C(CH_3)_3$	−1.27	1.39	34
2	$CH(CH_3)_2$	−1.26	1.29	34
3	CH_2CH_3	−1.25	1.18	34
4	$(CH_2)_3CH_3$	−1.26	1.13	34
5	CH_3	−1.24	0.94	34
6	C_6H_5	−1.22	0.89	34
7	$C_2H_2(C_6H_5)$	−1.24	0.85	34
8	C_6F_5	−1.20	0.67	39
9	C_6F_4H	−1.20	0.61	39
10	$C_2(C_6H_5)$	−1.06	0.57	34
11	ClO_4^-	−1.02	0.57	61
12	Cl^-	−1.09	0.55	64
13	$N_3C_2(CO_2CH_3)_2$	−1.02	0.54	this work
14	N_3^-	−1.05	0.53	this work
15	$N_4C(CH_2CH_3)$	−1.00	0.51	this work
16	CN^-	−1.05	0.50	this work
17	$N_4C(C_6H_5)$	−1.08	0.47	this work
18	OAc^-	−1.12	0.45	64
19	$SO_3C_6H_5^-$	−1.07	0.34	64
20	$SO_3CH_3^-$	−1.07	0.33	64

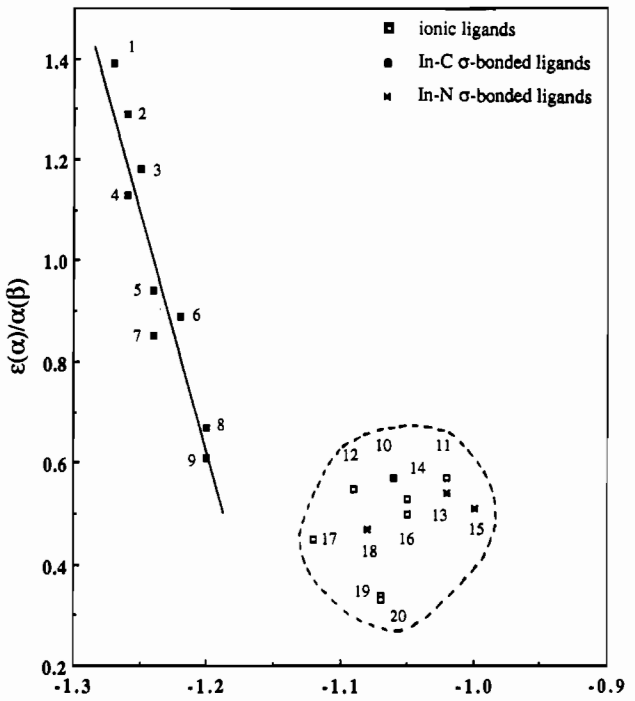

Figure 10. Correlation between half-wave potential and the ratio of $\epsilon(\alpha)/\epsilon(\beta)$ for different indium complexes. Data for compounds **1–20** are listed in Table XIV.

The above results suggest that the electrochemistry of the tetrazolato complexes is generally reversible in CH_2Cl_2 and can be represented as shown in eqs 1–4.

$$(P)In[N_4C(R)] + e^- \rightleftharpoons [(P)In[N_4C(R)]]^{\bullet-} \quad (1)$$

$$[(P)In[N_4C(R)]]^{\bullet-} + e^- \rightleftharpoons [(P)In[N_4C(R)]]^{2-} \quad (2)$$

$$(P)In[N_4C(R)] \rightleftharpoons [(P)In[N_4C(R)]]^{\bullet+} + e^- \quad (3)$$

$$[(P)In[N_4C(R)]]^{\bullet+} \rightleftharpoons [(P)In[N_4C(R)]]^{2+} + e^- \quad (4)$$

This behavior is quite different from that of the σ-bonded indium–carbon derivatives such as (P)In(CH_3) or (P)In(C_6H_5).[34] For example, a rapid cleavage of the axial metal–ligand bond is

not observed after electrooxidation of (P)In[$N_4C(R)$], as is the case for (P)In(R). In addition, half-wave potentials for the first reduction and first oxidation of (P)In[$N_4C(R)$] are not close to those of the σ-bonded carbon derivatives but rather are similar to those of ionic (P)InX species.[61] Moreover, as already noted, the UV-visible spectra of (P)In[$N_4C(R)$] are close to those of the ionic (P)InX derivatives.

Numerous correlations have been made between the redox and spectral properties of different metalloporphyrins. For example, the degree of axial-bond polarization has been related to the ratio of Q band molar absorptivity, $\epsilon(\alpha)/\epsilon(\beta)$, in the UV-visible spectra. This ratio is listed in Table XIV for indium tetraphenylporphyrin complexes with different axial ligands, and the resulting correlation between $E_{1/2}$ and spectral data is graphically presented in Figure 10. The value of $\epsilon(\alpha)/\epsilon(\beta)$ for (TPP)In[$N_4C(C_6H_5)$] is 0.47 and is similar to values measured for (TPP)InX where X = SO_3Ph^-, SO_3Me^-, Cl^-, OAc^-, N_3^-, CN^-, or ClO_4^- (see Table XIV). In contrast, the $\epsilon(\alpha)/\epsilon(\beta)$ ratios for the (P)In(R) complexes reflect a changeover of the metal-ligand bond from pure σ-bonded character when R = $C(CH_3)_3$ or $CH(CH_3)_2$ to an ionic-like character when R = $C_2C_6H_5$. This is reflected by the data in Figure 10, which clearly demonstrates that the tetrazolato and triazolato complexes both have an axial indium-nitrogen bond with ionic-like character.

Acknowledgment. The support of the CNRS, the National Science Foundation (Grants CHE-8515411 and INT-8412696), and NATO (Grant 0168/87) is gratefully acknowledged.

Supplementary Material Available: Tables of hydrogen atom fractional coordinates, anisotropic temperature factors, bond distances and angles, and least-squares planes (13 pages); a table of observed and calculated structure factors for (OEP)In[$N_4C(CH_3)$] (26 pages). Ordering information is given on any current masthead page.

Contribution from the Laboratoire de Synthèse et d'Electrosynthèse Organométalliques, associé au CNRS (URA 33), Faculté des Sciences "Gabriel", 6, Boulevard Gabriel, 21100 Dijon, France, Department of Chemistry, University of Houston, Houston, Texas 77204-5641, and Laboratoire de Minéralogie et Cristallographie associé au CNRS (URA 809), Université de Nancy I, BP 239, 54506 Vandoeuvre les Nancy, France

Metalloporphyrins Containing σ-Bonded Nitrogen Axial Ligands. 2. Synthesis and Characterization of Iron(III) Tetrazolato and Triazolato Porphyrin Complexes. Molecular Structure of (5-Methyltetrazolato)(2,3,7,8,12,13,17,18-octaethylporphinato)iron(III)

R. Guilard,*[1a] I. Perrot,[1a,b] A. Tabard,[1a] P. Richard,[1a] C. Lecomte,[1c] Y. H. Liu,[1b] and K. M. Kadish*[1b]

Received June 11, 1990

The first synthesis and characterization of iron(III) porphyrins with σ-bonded tetrazolato or triazolato axial ligands are reported. These compounds are represented as (P)Fe[$N_4C(R)$] or (P)Fe($N_3C_6H_4$) where P = the dianion of octaethylporphyrin (OEP) or tetramesitylporphyrin (TMP) and R = C_6H_5, *p*-$CH_3C_6H_4$, *m*-$CH_3C_6H_4$, CH_3, or CH_2CH_3. Each metalloporphyrin may exist in two different isomeric forms, which are labeled as isomer I and isomer II for the case of (P)Fe[$N_4C(R)$]. The linkage mode of the tetrazolato group (and the type of isomer) was determined for two representative complexes by single-crystal X-ray diffraction. (OEP)Fe[$N_4C(CH_3)$]·$^1/_2C_6H_5CH_3$ crystallizes as isomer I in the monoclinic system, space group $P2_1/c$ (a = 15.967 (2) Å, b = 17.464 (4) Å, c = 14.726 (2) Å, β = 66.59 (2)°, Z = 4, V = 3765 Å^3, ρ = 1.27 g cm^{-3}, $R(F)$ = 5.97%, $R_w(F)$ = 5.82%). (OEP)Fe[$N_4C(C_6H_5)$] also crystallizes in the monoclinic space system, space group $P2_1/c$ (a = 12.798 (2) Å, b = 12.748 (3) Å, c = 24.301 (5) Å, β = 78.93 (2)°, Z = 4, V = 3891 Å^3, ρ = 1.25 cm^{-3}) but exists as isomer II. Altogether, eight different tetrazolato and triazolato complexes were synthesized, and each was characterized by UV-visible, IR, ESR, and ^{1}H NMR spectroscopy, as well as by electrochemistry. Variable-temperature magnetic susceptibility measurements were also performed and give data consistent with a high-spin-state Fe(III) central metal. An analysis of the isotropic chemical shifts shows that the electronic structures of the high-spin-state complexes are virtually independent of the specific σ-bonded nitrogen axial ligand.

Introduction

Numerous papers have been devoted to a characterization of organic and inorganic azide reactivity. Organic azides can react with nitriles, alkenes, or alkynes to give tetrazoles, triazolines, or triazoles,[2-5] while inorganic azides can react with dipolarophiles to give as a final product a metal-nitrogen-bonded heterocycle.[6-22]

Chart I

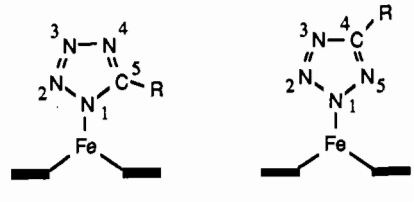

ISOMER I ISOMER II

Recently, these classical reactions have been utilized to synthesize main-group or transition-metal metalloporphyrins with σ-bonded

(1) (a) Université de Bourgogne. (b) University of Houston. (c) Université de Nancy I.
(2) L'Abbé G. *Chem. Rev.* **1969**, *69*, 345 and references therein.
(3) Patai, S. *The Chemistry of Azido Group*; Interscience: New York, 1971.
(4) Huisgen, R. In *1,3-Dipolar Cycloaddition Chemistry*; Padwa, A., Ed.; Interscience: New York, 1984; Vol. I, Chapter I.
(5) Scriven, E. F. V. *Azides and Nitrenes, Reactivity and Utility*; Academic: Orlando, FL, 1984.
(6) Beck, W.; Fehlhammer, W. P. *Angew. Chem., Int. Ed. Engl.* **1967**, *6*, 169.
(7) Beck, W.; Fehlhammer, W. P.; Bock, H.; Bauder, M. *Chem. Ber.* **1969**, *102*, 3637.
(8) Beck, W.; Burger, K.; Fehlhammer, W. P. *Chem. Ber.* **1971**, *104*, 1816.
(9) Weis, J. C.; Beck, W. *Chem. Ber.* **1972**, 105, 3203.
(10) Fehlhammer, W. P.; Kemmerich, T.; Beck, W. *Chem. Ber.* **1979**, *112*, 468.
(11) Kreutzer, P. H.; Weis, J. C.; Bock, H.; Erbe, J.; Beck, W. *Chem. Ber.* **1983**, *116*, 2691.
(12) Fehlhammer, W. P.; Beck, W. *Z. Naturforsch.* **1983**, *38B*, 546.
(13) Ziolo, R. F.; Thich, J. A.; Dori, Z. *Inorg. Chem.* **1972**, *11*, 626.
(14) Dori, Z.; Ziolo, R. F. *Chem. Rev.* **1973**, *73*, 247.
(15) (a) Sato, F.; Etoh, M.; Sato, M. *J. Organomet. Chem.* **1972**, *37*, C51. (b) *Ibid.* **1974**, *70*, 101.
(16) Rosan, A.; Rosenblum, M. *J. Organomet. Chem.* **1974**, *80*, 103.
(17) Busetto, L.; Palazzi, A.; Ros, R. *Inorg. Chim. Acta* **1975**, *13*, 233.
(18) Rigby, W.; Bailey, P. M.; McCleverty, J. A.; Maitlis, P. M. *J. Chem. Soc., Dalton Trans.* **1979**, 371.
(19) La Monica, G.; Ardizzoia, G.; Cenini, S.; Porta, F. *J. Organomet. Chem.* **1984**, *273*, 263.

0020-1669/91/1330-0027$02.50/0